System identification of a dynamical model of a vehicle using data generated by a high-fidelity simulator

Chenxi Zhang

Master of Science Thesis

TU Delft Delft University of Technology

Delft Center for Systems and Control

System identification of a dynamical model of a vehicle using data generated by a high-fidelity simulator

Master of Science Thesis

For the degree of Master of Science in Systems and Control at Delft University of Technology

Chenxi Zhang

February 10, 2021

Faculty of Mechanical, Maritime and Materials Engineering (3mE) · Delft University of Technology

Delft University of Technology
Department of
Delft Center for Systems and Control (dcsc)

The undersigned hereby certify that they have read and recommend to the Faculty of Mechanical, Maritime and Materials Engineering (3mE) for acceptance a thesis entitled

System identification of a dynamical model of a vehicle using data generated by a high-fidelity simulator

by

Chenxi Zhang

in partial fulfillment of the requirements for the degree of

Master of Science Systems and Control

Dated: February 10, 2021

Supervisor(s):

Dr. R. Ferrari

Reader(s):

Dr. Manuel Mazo

T. Keijzer

Abstract

Unmanned vehicles are a vital topic in today's science and technology field. The safety problem of unmanned vehicles has been paid more attention from researchers. People are continually developing new control technologies, making the auxiliary driving or control of vehicles more accurate and reliable. Before designing a reliable controller, researchers need to obtain an accurate model of the vehicle system. However, the vehicle is a complex system, and various vehicle parameters are difficult to obtain by direct sensor measurement. In addition, there are deviations between the actual vehicle and the simulation model. At this time, it is necessary to make system identification to obtain reliable vehicle parameters and models.
In this paper, vehicle simulation is carried out based on the CarSim C-Class model under the environment of CarSim vehicle simulation software. The model includes tire, suspension, steering, driver, and other subsystems. This platform can simulate a vehicle closed to the real one. The vehicle model can be controlled through Simulink and output the real-time data of various variables of the vehicle system. Then, the data required for identification and validation can be obtained through the joint simulation of CarSim and Simulink.
By comparing different vehicle and tire models, different identification data sets and different algorithms, this paper summarizes the advantages and disadvantages of different choices and their applicability. First, the comparison between the bicycle model and the four wheels vehicle model is implemented. The Interior-point algorithm was used to identify the two models under different control data sets. The results of parameter validation and vehicle validation are analyzed.
Then, under the same control data set, the four wheels model is selected for the comparative experiment between different algorithms. The first comparison with the Interior-point algorithm is the Unscented Kalman Filter (UKF) and its improved method Particle Swarm Optimization-Unscented Kalman Filter (PSO-UKF). The Magic Formula tire model was then identified by Genetic Algorithm (GA) algorithm, which compares with the Dugoff tire model. Each model and algorithm has its suitable scenarios. Also different data sets lead to various result. The analysis and application suggestions of different algorithms, data sets and models will be given in the end.

Table of Contents

List of Figures

List of Tables

Preface

Looking back on the past year, I am delighted that I could complete this project and gain the necessary knowledge and exercise.
This project was forced to change from a laboratory project to a simulation project because of the Covid-19 epidemic.
Thanks to my supervisor Dr. R. Ferrari, who helped me complete the transformation of the project and helped me solve the challenges in the project. I also want to thank my parents for letting me go back to my hometown before the epidemic breakout in the Netherlands to ensure my safety and providing me with quiet and comfortable study environment at home.

Chapter 1

Introduction

1-1 Project Background

In the field of systems and control, various algorithms are used to control machine to operate stably, accurately and rapidly. This has very high requirements for the control algorithm. For example, the control system needs to have a fast response speed, small overshoot, and no steady-state error. At the same time, the system should also have robustness and anti-interference ability [5]. Therefore, before designing the control system, the precise mathematical model of the system must be mastered, and system identification plays this role.
The system identification uses statistical methods to construct dynamic systems' mathematical models from measured data [6]. System identification also includes identification algorithm selection and the optimal design of experiments to generate data set to fit such models effectively.
When doing vehicle design and control, The accuracy of parameters plays an important role in dynamic modeling and control of a vehicle, such as mass, the moment of inertia, stiffness. Such parameters' uncertainty will have serious adverse effects on the acceleration and braking performance and steering stability, which would lead to a decline in safety. Given the limitation of sensors, it is hard to measure the value of some states directly. As a result, the vehicle dynamical parameters identification is the top priority of vehicle control.
For vehicle parameters identification, the commonly used method are least-square optimization [7][8], Kalman Filter (KF)[9][10], and neural network[11]. Other optimization methods can also be used to do identification similar as least-square optimization, such as Interior-point method. Moreover, Genetic Algorithm (GA)[3] and Particle Swarm Optimization (PSO)[12] can be used to solve problems with high dimension or multiple local optimums.
In this project, the Interior-point algorithm and the Unscented Kalman Filter (UKF) are implemented to identify the vehicle's parameters. The PSO method is combined with the UKF. The GA identify the parameters of the Magic Formula.

1-2 Project Goals

The goal of this project will be divided into the following parts. Firstly, a vehicle's full identification cycle will be practiced in the bicycle vehicle model and four wheels vehicle model scenarios by using Interior-point algorithm with different data sets. The difference between simplified and complex models, the result from different data sets, and the validation results will be studied.
Secondly, some other algorithms such as UKF, Particle Swarm Optimization-Unscented Kalman Filter (PSO-UKF), and GA will also be implemented. The results will be analyzed and compared.
The conclusion of data set, model, and algorithm selection is given by analyzing the results of the experiments.

1-3 Vehicle Simulation Platform

In this project, CarSim is used to simulate a real vehicle. CarSim delivers the most accurate, detailed, and efficient methods for simulating the performance of passenger vehicles and light-duty trucks. With twenty years of real-world validation by automotive engineers, CarSim is universally the preferred tool for analyzing vehicle dynamics, developing active controllers, calculating a car's performance characteristics, and engineering next-generation active safety systems [13].

1-4 Report Structure

This thesis will be introduced in the following chapters. The tire model and vehicle model are introduced in Chapter 2. Chapter 3 discusses data acquisition from CarSim and data processing method. The experiments and analysis of parameter identification by Interior-point method are shown in Chapter 4 and the experiments and analysis by other methods such as UKF and GA are introduced in Chapter 5. The conclusions and recommendations are given in the last part, Chapter 6.

Chapter 2

Vehicle Modeling

Before implemented the identification algorithms, the physical model should be formulated. The vehicle is simulated as an object in space, which is composed of many separate parts in a three-dimensional space and has a high degree of freedom. After simplification, it can be processed as a three-degree-of-freedom model (3-DOF) system.
There are generally two methods to construct a vehicle model: the kinetic and dynamic methods. The dynamic method can better describe the dynamic performance by analyzing the equation relation between the force and acceleration of the vehicle, and it is chosen for this project. Also, some components, such as the tire model, are required when constructing a vehicle model and will be given in the next section.
This chapter refers to the book "Vehicle dynamics and control" [14].

2-1 Tire Model

Tires are the only part of the vehicle that comes into contact with the ground. They drive, brake, and steer the vehicle by acting force against the ground. Therefore, the tire model is one of the essential parts of vehicle simulation. Tire models describe the longitudinal, lateral forces and moments generated by the wheel motion under different force and slip conditions. There are many different types of tire models being used. Usually, models can be distinguished as theoretical models based on physics of the tire construction[15][16], and empirical or semi-empirical models based on experimental results[17][18]. Also, combinations of both approaches are used in the development of the tire model[3]. The Magic Formula and the Dugoff model will be studied in this thesis.

2-1-1 Magic Formula

The Magic Formula tire model was proposed by Professor H.B.Pajejka of Delft University of Technology in the Netherlands in 1987. It is a semi-empirical tire model based on experimental data.

The tire test data are fitted by trigonometric function combination, and a set of models with the same form can express the tire longitudinal force, lateral force and moment.
The equations of Magic Formula reference the paper "An Alternative Method to Determine the Magic Tyre Model Parameters Using Genetic Algorithms" [3] and "The Magic Formula Tyre Model" [17].
The Magic Formula [17] at pure slip conditions is expressed as:

$$y(x) = D \cdot sin[C \cdot arctan\{B \cdot x - E \cdot (B \cdot x - arctan(B \cdot x))\}] \tag{2-1}$$

where:

$$\begin{aligned} Y_{pure}(X) &= y(x) + S_v \\ x &= X + S_h \end{aligned} \tag{2-2}$$

Where the output variable Y_{pure} represents the braking and traction force F_x when the input variable X represents the longitudinal slip ratio λ and Y_{pure} represents the lateral force F_y when the input variable X represents the slip angle α[3]. S_v represents horizontal shift and S_h represents vertical shift which are set as zero in this project.
Slip ratio is the difference value between the actual distance traveled by the tire and the equivalent distance of the tire's rotation for a time unit divided by the larger value in between which can be denoted as:

$$\lambda = \frac{\omega \cdot r_{wheel} - u}{max(\omega \cdot r_{wheel}, u)} \tag{2-3}$$

Slip angle is the difference between steering angle and the actual heading angle which can be denotes as Fig. 2-1.

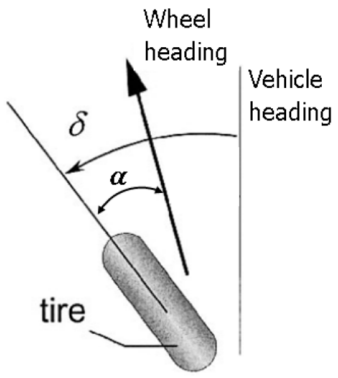

Figure 2-1: Angle information of tire movement

Eq. 2-1 can produce characteristic forces F_y and F_x, which closely match the measurement curve, as functions of their respective slips: slip Angle α and longitudinal slip ratio λ under the action of load F_z [1]. The curve reflects the geometry information of the Magic Formula is shown in Fig. 2-2.
The coefficient D represents the peak value and the product BCD denotes the slope at the

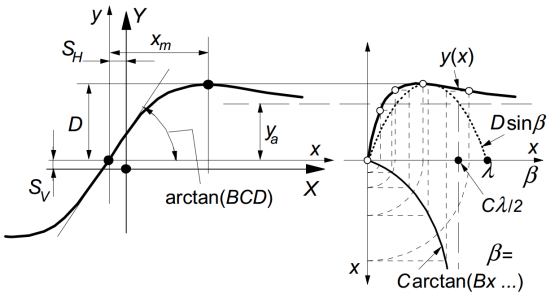

Figure 2-2: Curve produced by Magic Formula [1]

origin. C controls the limits of the range of sine function appearing in eq. 2-1. E controls the horizontal position of the peak [1].
Weighting functions G are introduced which multiplied with original pure slip functions produce the combined effects of λ on F_x and of α on F_y[3], so the Magic Formula at combined slip conditions is expressed as:

$$Y_{combined}(X) = G(x) \cdot Y_{pure}(X) + S_v \tag{2-4}$$

The coefficients for each tire characteristic are expressed as follows and their meaning is presented at Pacejka [17]:
where the coefficients for pure longitudinal characteristic are presented at Pacejka[17] as:

$$\begin{aligned} D &= (PDX1 + PDX2 \cdot df_z) \cdot F_z \\ C &= PCX1 \\ E &= (PEX1 + PEX2 \cdot df_z + PEX3 \cdot df_z^2) \cdot (1 - PEX4 \cdot sgn(\lambda + S_{hx})) \\ B \cdot C \cdot D &= F_z \cdot (PKX1 + PKX2 \cdot df_z) \cdot e^{-PKX3 \cdot df_z} \\ B &= \frac{B \cdot C \cdot D}{C \cdot D} \\ S_{hx} &= (PHX1 + PHX2 \cdot df_z) \\ S_{vx} &= F_z \cdot (PVX1 + PVX2 \cdot df_z) \end{aligned} \tag{2-5}$$

where F_z represents the vertical force and df_z is the notation for the non-dimensional increment of the vertical load with respect to the (adapted) nominal load [1].

The weighting function G for combined longitudinal force is:

$$\begin{aligned} G(\alpha) &= \frac{cos(C_\alpha \cdot arctan(B_\alpha \cdot (\alpha + S_{h\alpha})))}{cos(C_\alpha \cdot arctan(B_\alpha \cdot S_{h\alpha})}) \\ C_\alpha &= RCX1 \\ B_\alpha &= RBX1 \cdot cos(arctan(RBX2 \cdot \lambda)) \\ S_{h\alpha} &= RHX1 \end{aligned} \tag{2-6}$$

and for combined lateral force, where the coefficients for pure lateral characteristic are pre-

sented at Pacejka [17] as:

$$\begin{aligned} D &= (PDY1 + PDY2 \cdot df_z) \cdot F_z \\ C &= PCY1 \\ E &= (PEY1 + PEY2 \cdot df_z) \cdot (1 - PEY3 \cdot sgn(\alpha + S_{hy})) \\ B \cdot C \cdot D &= PKY1 \cdot F_{z0} \cdot sin(2 \cdot arctan(\frac{F_z}{PKY2 \cdot F_{z0}})) \\ B &= \frac{B \cdot C \cdot D}{C \cdot D} \\ S_{hy} &= (PHY1 + PHY2 \cdot df_z) \\ S_{vy} &= F_z \cdot (PVY1 + PVY2 \cdot df_z) \end{aligned} \tag{2-7}$$

the weighting function G for combined lateral force is:

$$\begin{aligned} G(\lambda) &= \frac{cos(C_\lambda \cdot arctan(B_\lambda \cdot (\lambda + S_{h\lambda})))}{cos(C_\lambda \cdot arctan(B_\lambda \cdot S_{h\lambda}))} \\ C_\lambda &= RCY1 \\ B_\lambda &= RBY1 \cdot cos(arctan(RBY2 \cdot (\alpha - RBY3))) \\ S_{h\lambda} &= RHY1 + RHY2 \cdot df_z \\ D_{v\lambda} &= D \cdot (RVY1 + RVY2 \cdot df_z) \cdot cos(arctan(RVY4 \cdot \alpha)) \\ S_{v\lambda} &= D_{v\lambda} \cdot sin(RVY5 \cdot arctan(RVY6 \cdot \lambda)) \end{aligned} \tag{2-8}$$

Figure of longitudinal force as a function of slip ratio is shown in Fig. 2-3. It goes up linearly, then it goes down slowly after reaches the summit and end with a almost constant force. In CarSim, the tire model is also constructed according to the Magic Formula. However, as the Magic Formula requires more than 30 parameters to be identified for a single tire, it is obviously very difficult for the identification algorithm to process the high dimensional data. This requires a trade-off between precision and computation. In the second half of the report, Genetic Algorithm (GA) is tried to identify the Magic Formula parameters.

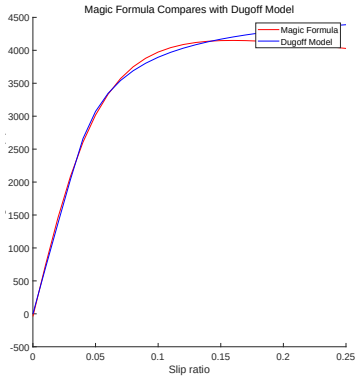

Figure 2-3: Slip ratio-longitudinal curves of Magic Formula and Dugoff Model

2-1-2 Dugoff Model

The Dugoff model is widely used in vehicle identification and simulation. The model uses a series of variables such as tire longitudinal slip ratio, slip Angle and cornering stiffness to describe the longitudinal and lateral friction of tires, which has the advantages of simple equation, low computational load and suitable for multi-lateral/longitudinal working conditions [19]. The Dugoff model can be denoted as [20]:

$$\begin{aligned} F_x &= \frac{C_\lambda\ \lambda}{1-\lambda} f(\zeta) \\ F_y &= \frac{C_\alpha\ tan(\alpha)}{1-\lambda} f(\zeta) \\ \zeta &= \frac{\mu_{max} F_z (1+\lambda)}{2\sqrt{(C_\lambda \lambda)^2 + (C_\alpha tan(\alpha))^2}} \\ f(\zeta) &= \begin{cases} (2-\zeta), \zeta < 1 \\ 1, \zeta \geq 1 \end{cases} \end{aligned} \tag{2-9}$$

where F_x = longitudinal forces of tires(N)
F_y = lateral forces of tires (N)
C_λ = longitudinal stiffness of tires (N/rad)
C_α = lateral stiffness of tires (N/rad)
α = side slip angle of tires (rad)
λ = longitudinal slip ratio of tires
μ_{max} = maximum friction coefficient.

The comparison between Dugoff model and Magic Formula is shown in Fig. 2-3. As can be seen, the force changing can be divided in two sections, which are linear section and minor changing to almost constant section. It doesn't have decrease section comparing to Magic Formula model. In reality, vehicle tires usually slip within a small section to keep stability and control, where the Dugoff model can describe the tire system very well. Moreover, the Dugoff model only needs to identify three parameters for a single tire, which can effectively reduce the coupling of parameters and reduce the computational load for the overall identification of vehicles. In the following system identification, this project will mainly use the Dugoff model.

2-1-3 Simplified Tire Model

Both the Dugoff model and Magic Formula are nonlinear models. When a linear model is required for the system, the tire model also needs to be simplified. Fortunately, tire models can be mostly represented by linear equations within the range of stable operation, as shown in Fig. 2-4. So in this project, the tire model in the bicycle model study is represented by the following formula.

$$\begin{aligned} F_x &= C_\lambda \cdot \lambda \\ F_y &= C_\alpha \cdot \alpha \end{aligned} \tag{2-10}$$

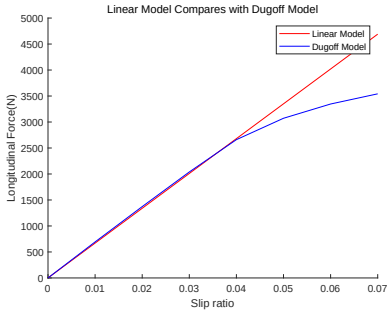

Figure 2-4: Slip ratio-longitudinal curves of Dugoff and linear model

2-2 Vehicle Dynamic Model

2-2-1 Bicycle Model

In the process of vehicle simulation or identification, the bicycle model is usually firstly studied. The bicycle model is a simplified version of the vehicle model, which combines the left and right wheels into one. It can be approximated by linear state space equations. The plot is shown in Fig. 2-5.

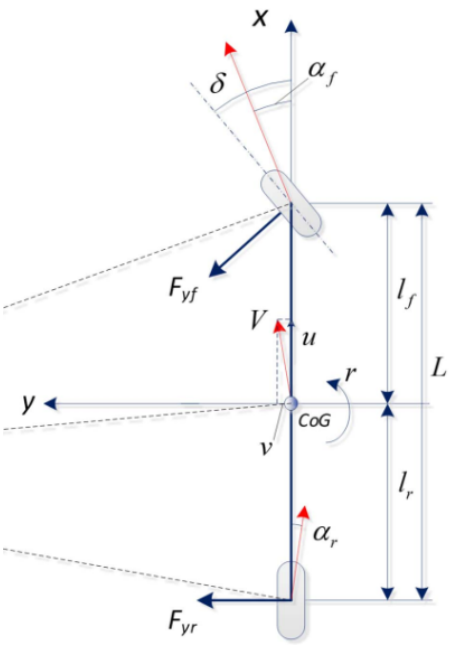

Figure 2-5: The bicycle model

The ideal vehicle dynamic model can be represented by a differential equation. This model

depends on Newton Laws, D'Alembert's principle, Lagrange principle, etc.
The dynamic model is based on differential equation which is expressed as the function of velocities, yaw rate, moment of inertial, etc [21].

$$\begin{aligned} ma_x &= m(\dot{u} - vr) = \sum F_x = F_{xf}cos\delta - F_{yf}sin\delta + F_{xr} - F_{air} \\ ma_y &= m(\dot{v} + ur) = \sum F_y = F_{xf}sin\delta + F_{yf}cos\delta + F_{yr} \\ I_z\dot{r} &= \sum M_z = l_f(F_{xf}sin\delta + F_{yf}cos\delta) - l_rF_{yr} \end{aligned} \tag{2-11}$$

where a_x and a_y are the longitudinal and lateral acceleration, u and v are the longitudinal and lateral velocity, F_{xf} and F_{yf} are the longitudinal and lateral forces of front wheel, F_{xr} and F_{yr} are the longitudinal and lateral forces of rear wheel. F_{air} is the longitudinal air friction which can be calculated by eq. 2-12. δ is the steering angle, I_z is the yaw inertia, r is the yaw rate, M_z is the moment acting on COG, l is the length of the vehicle, l_r and l_f are the distance between COG and the corresponding axles. The steering angle δ usually is within a small amount, so to keep the system simple, $cos\delta$ is approximated as 1 and $sin\delta$ is approximated as 0.
The longitudinal air friction can be calculated as:

$$F_{air} = C_{air} \cdot u^2 \tag{2-12}$$

where C_{air} is the air friction coefficient. The front and rear slip angle can be denoted as:

$$\alpha_f = \delta_f - \frac{v + l_f r}{u} \tag{2-13}$$

$$\alpha_r = \delta_r - \frac{v - l_r r}{u} \tag{2-14}$$

Then eq. 2-13 and eq. 2-14 can be taken into eq. 2-10 to calculate the lateral forces F_y.

Eq. 2-3 can be taken into eq. 2-10 to calculate the lateral forces F_x.

2-2-2 Four Wheels Model

Although the bicycle model is simple and practical, in some cases it cannot meet the requirements of accuracy. In order to achieve higher accuracy for yaw movement estimation, four wheels model is very necessary as shown in Fig. 2-6.

The formula for the four wheels model is very similar to that for the bicycle model, as shown below:

$$\begin{aligned} ma_x &= m(\dot{u} - vr) = \sum F_x = F_{xfl} + F_{xfr} + F_{xrl} + F_{xrr} - F_{air} \\ ma_y &= m(\dot{v} + ur) = \sum F_y = F_{yfl} + F_{yfr} + F_{yrl} + F_{yrr} \\ I_z\dot{r} &= \sum M_z = l_f(F_{yfl} + F_{yfr}) - l_r(F_{yrl} + F_{yrr}) - B_l(F_{xfl} + F_{xrl}) + B_r(F_{xfr} + F_{xrr}) \end{aligned} \tag{2-15}$$

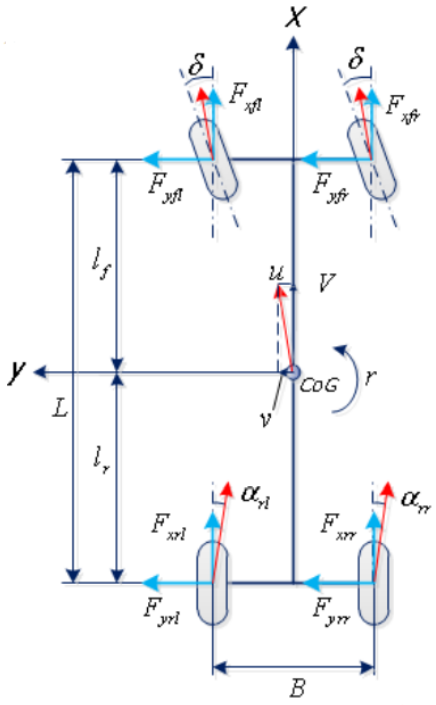

Figure 2-6: The four wheels vehicle model

where B_r represents the distance between the center of right wheel to the COG and B_l represents the distance between the center of left wheel to the COG. F_{xi} and F_{yi} can be denoted by the following equation.

$$\begin{bmatrix} F_{xi} \\ F_{yi} \end{bmatrix} = \begin{bmatrix} cos\delta_i & -sin\delta_i \\ sin\delta_i & cos\delta_i \end{bmatrix} \begin{bmatrix} F_{xwi} \\ F_{ywi} \end{bmatrix}, \ i = fl, \ldots, rr \tag{2-16}$$

where F_{xwi} and F_{ywi} are the lateral and longitudinal force of each tire in the tire coordinate. The slip angle calculation also needs to be slightly modified as:

$$\begin{aligned} \alpha_{fl} &= \delta_{fl} - \frac{v + l_f r}{u - \frac{B_l}{2} r} \\ \alpha_{fr} &= \delta_{fr} - \frac{v + l_f r}{u + \frac{B_r}{2} r} \\ \alpha_{rl} &= \delta_{rl} - \frac{v - l_r r}{u - \frac{B_l}{2} r} \\ \alpha_{rr} &= \delta_{rr} - \frac{v - l_r r}{u + \frac{B_r}{2} r} \end{aligned} \tag{2-17}$$

In order for the vehicle to steer smoothly, the circle center of steering angle of each tire should be at the same point, which requires the Ackermann geometry shown as Fig. 2-7.

Most steering systems on cars and light trucks only have 50% to 75% of Ackermann steer [22].

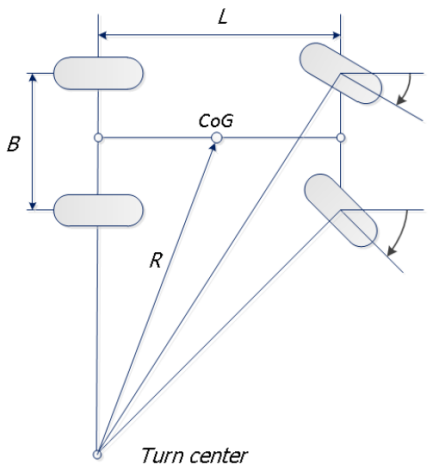

Figure 2-7: The Ackermann geometry

2-3 Conclusion

This chapter describes the commonly used vehicle and tire models that can be selected for subsequent system identification algorithms. It is very important to construct an accurate vehicle system model for simulation or identification. A detailed vehicle model will have dozens of degrees of freedom, which requires a very high amount of computation and a lot of sensors to obtain information. Practically, such a complex and sophisticated model is generally not required. So the trade-off between computational complexity and model accuracy need to be considered, therefore, the bicycle model and the four wheels model are widely used and adopted by this project. Similarly, a tire model also requires a trade-off between complexity and accuracy. In the following experiments, this project will identify and compare vehicle models and tire models of different complexity.

Chapter 3

Data Acquisition and Processing

In the vehicle system identification experiment, the vehicle's position, speed, acceleration, forces, and other information need to be acquired through the sensor. Since the experiment requires high precision for some measurements, such as the slip ratio and slip angle values, which are very small, the tiny errors in the measurements may also lead to a substantial error in the final experimental results. Therefore, the noises of the sensors need to be within a minimal range, and the signal also needs to be filtered before it can be used. In this project, the simulation software CarSim was used to simulate as an actual vehicle. Meanwhile, noises are added to some key variables to get close to the real-life situation. This chapter provides a brief introduction to CarSim and how to use it, as well as data processing related issues.

3-1 CarSim Introduction

CarSim is a simulation software that can predict the vehicle's response to driver control in different road geometry, friction, wind, and other environments. The software simulates physical tests with mathematical models, allowing engineers to see results similar to the real vehicle test results, but that can be repeated, safely, and faster than physical tests. They include the state and response of the tire when it comes into contact with the road, and how the force of the tire/road interface is transferred to the chassis through the suspension, etc. Manufacturers have repeatedly validated these models to reproduce the overall vehicle motion needed to assess handling, directional and rolling stability, braking, and acceleration [13].

3-2 CarSim-Simulink Co-simulation

CarSim can co-simulate with Simulink. CarSim can pass the model to Simulink, and the corresponding CarSim package can be used in Simulink for simulation. Input parameters, output parameters, road conditions, and driver models can be set in the CarSim. In Simulink, control signals can be sent to the CarSim package, and output information can be obtained for

further calculation. As shown in Fig. 3-1

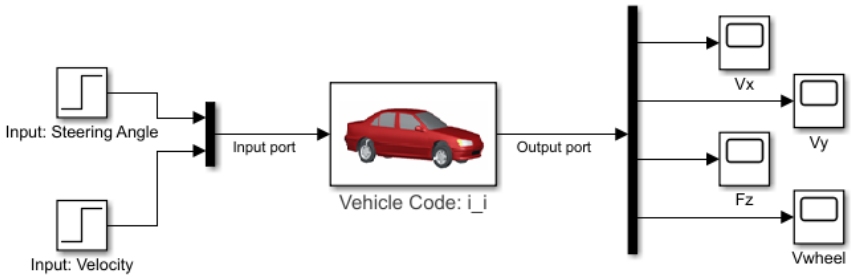

Figure 3-1: CarSim-Simulink co-simulation

3-3 Data Processing

In this project, the sampling frequency is 10. This frequency is far less than half of the system's highest response frequency, which conforms to the Shannon sampling theorem. In order to simulate similar to the real situation of vehicles, white noise was added to the three main signals, longitudinal and lateral forces, u (Longitudinal Velocity), v (Lateral Velocity), and r (Yaw rate). The standard deviation of the noises are between 0.1% to 5% of the average value depending on the characteristics of the system. Therefore, a filter is needed to process the signal to reduce noises interference.
Because the mean of noise is 0, and the signals are continuous, the change at the adjacent sampling points can be ignored. The appropriate filter is smoothing filter. An averaging method is adopted, and the average value of adjacent points is calculated as the value of this point. The range is plus or minus two sampling points.

3-4 Conclusion

This chapter introduces how to obtain vehicle data through CarSim-Simulink co-simulation. In the following sections, the data used for identification and validation comes from this emulator. The vehicle can be driven in a straight line or change the direction and velocity according to different identification requirements.
At the same time, in order to make the experiment close to the real-life situation, white noises are added in some data sets. The smoothing filter is used to process the signal before the system identification.

Chapter 4

Vehicle Identification by Interior-point Algorithm

System identification is based on the system's input and output functions in time or frequency domain to determine the mathematical model describing the system's behavior. The purpose of establishing a mathematical model through identification is to estimate parameters that characterize the behavior of the system, to build a model that mimics the behavior of a system in real life, to predict the future evolution of system output using the current measurable system inputs and outputs, and to design controllers. The main problem of analyzing the system is to determine the output signal according to the input time function and the characteristics of the system.
There are plenty of identification methods. Optimization Algorithms and Kalman Filter (KF) are commonly used, and neural networks have developed rapidly to solve complex problems. In this chapter, the identification problem is transferred into optimization problem and the Interior-point algorithm is used to identify the parameters of a vehicle. Some algorithms have also been tested as comparison and are also introduced in Chapter 5, such as Unscented Kalman Filter (UKF), Particle Swarm Optimization (PSO) and Genetic Algorithm (GA).

4-1 Interior-point Algorithm

The nonlinear optimization algorithm is the most commonly used system identification method because system identification can usually be transformed into a nonlinear optimization problem. It uses the difference between the estimated value and the real value as the cost function to find the parameter value that makes the error function approach zero.
For an unconstrained optimization problem, we can use the Newton method and other methods to solve it. When facing a constrained problem, we often need more advanced algorithms. Simplex Method can be used to solve linear programming propositions with constraints, Active Set Method can be used to solve quadratic programming with constraints, and Interior-point

Method is another method used to solve nonlinear optimization problems with constraints. For system parameter identification, the range of some parameters can often be estimated, so the constrained optimization algorithm can be applied in this field. According to the experimental results, the Interior-point method has a good performance as an optimization algorithm for system identification. So it is used in this experiment as the identification method.
Interior-point method with barrier function is introduced as following [23].
For a optimization problem:

$$\begin{aligned} &min\ f_0(x) \\ &subject\ to\ f_i(x) \leq 0,\ i = 1, \ldots, m \\ &Ax = b \end{aligned} \tag{4-1}$$

where $f_0, \ldots f_m$ are differentiable convex functions. Meanwhile, the optimal solution of x^* exists, and the corresponding target function value is p^*. Furthermore, the existence of the optimal dual variable λ^* and ν^*, together with the original variable x^*, satisfies the KKT condition:

$$\begin{aligned} \nabla f_0(x^*) + \sum_{i=1}^{m} \lambda_i^* f_i(x^*) + A^T \nu^* &= 0 \\ Ax^* &= b \\ f_i(x) &\leq 0,\ i = 1, \ldots, m \\ \lambda^* &\geq 0 \\ \lambda_i^* f_i(x^*) &= 0,\ i = 1, \ldots, m \end{aligned} \tag{4-2}$$

The inequality constraint in KKT condition makes it difficult to solve this problem. Therefore, the idea of Barrier Method is to replace the inequality constraint by adding an penalty function to the original objective function, which makes eq. 4-1 look like the following:

$$\begin{aligned} &min\ f_0(x) + \sum_{i=1}^{m} -(1/t) log(-f_i(x)) \\ &subject\ to\ Ax = b \end{aligned} \tag{4-3}$$

where $-(1/t)log(-f_i(x))$ is the barrier function and the value of the function is zero when no constraint is violated, and infinity when the constraint is violated.
Then define the logarithmic barrier as:

$$\phi(x) = -\sum_{i=1}^{m} log(-f_i(x)) \tag{4-4}$$

and the objective function becomes:

$$\begin{aligned} &min\ tf_0(x) + \phi(x) \\ &subject\ to\ Ax = b \end{aligned} \tag{4-5}$$

The central path of $x^*(t)$ is defined as:

$$x^*(t) = arg\min_x (tf_0(x) + \phi(x)) \tag{4-6}$$

$x^*(t)$ converge to x^* for $t \to \infty$. But the computational load also increases, so an appropriate t should be obtained iteratively. This is proved in the book "Convex optimization" [23].
As shown in 4-5, the inequality constraint optimization problem is transferred into equality constraint optimization problem, for which the optimum can be calculated as Sequential Quadratic Programming [24].
The optimization procedures are shown as the following: Given feasible x, and $t := t^{(0)>0}$, $\mu > 1$, tolerance $\epsilon > 0$.
repeat

1. Centering step. Compute $x^*(t)$ by minimizing $tf_0 + \phi$, subject to $Ax = b$, starting at x.
2. Update. $x := x^*(t)$.
3. Stopping criterion. Quit if $m/t < \epsilon$
4. Increase t. $t = \mu t$

Using Interior-point method to do Identification The ideal is to minimize the difference between estimated value and measured value.
Assume there are m (input, output) points:

$$(x_1, y_1), (x_2, y_2), \ldots, (x_m, y_m)$$

and a function:

$$y = f(x, \theta) \tag{4-7}$$

where θ is the unknown parameter vector which has n elements and $(m \gg n)$. The goal is to find the optimal set of θ to minimize the norm of the residual terms.

$$S = \sqrt{\sum_{i=1}^{m} r_i^2} \tag{4-8}$$

where $r_i = y_i - f(x_i, \theta)$

With the CarSim simulator, we can obtain real-time information about various variables, from which we can select some variables to be used in the identification system. The variables that can be used: tire vertical force F_z, steering angle δ, longitudinal velocity u, lateral velocity v, yaw rate r, and the wheel spinning speed V_{spin}.
In the following sections, the identification experiments by Interior-point method and its results as well as the corresponding validation results are introduced.

4-2 Internal Parameters Identification

Before implementing complex algorithms, some parameter can be calculated easily by the vertical force. The mass and center of gravity (COG) of a vehicle system varies with different passenger load and fuel load. Therefore, mass and COG should be calculated at the beginning of each driving maneuver.
Mass m, front and rear length l_f and l_r, and left and right width B_l and B_r can be identified

Vertical Force	F_{zfl}	F_{zfr}	F_{zrl}	F_{zrr}
Value(N)	4172	4260	2687	2767

Table 4-1: Vertical force for each wheel in a stationary state

by vertical force F_z in a stationary state of vehicle.

The distance between front and rear axle is $L = 2.578\ m$ and the distance between left and right wheel center is $B = 1.539\ m$ which can be measured easily. Then the position of COG can be represented by the distance between axle to COG and wheel to COG which can be calculated by vertical forces and the formula is shown in eq. 4-9.

$$\begin{aligned} l_f &= L\frac{F_{zrl}+F_{zrr}}{F_{zfl}+F_{zfr}+F_{zrl}+F_{zrr}} \\ l_r &= L - l_f \\ B_l &= B\frac{F_{zfr}+F_{zrr}}{F_{zfl}+F_{zfr}+F_{zrl}+F_{zrr}} \\ B_r &= B - B_r \end{aligned} \tag{4-9}$$

where l_f is the distance between front axle and COG, l_r is the distance between real axle and COG, B_l is the distance between left wheel center to COG, and B_r is the distance between right wheel center to COG.
The result is shown in Table 4-2

Symbol	l_f	l_r	B_l	B_r
Value(m)	1.0125	1.5665	0.7788	0.7602

Table 4-2: Distance between axles and wheels to COG

The mass of vehicle system can be calculated by $\sum F_z/9.8$ which is $1416.9kg$.

4-3 Bicycle Model Identification

The next step is to identify the parameters of simplified tire model, yaw inertia I_z and the air coefficient C_{air}. Experiments are divided into longitudinal maneuver and lateral maneuver from which the corresponding data required by identification can be obtained. In each subsection, the data acquisition, identification, validation, and result discussion are introduced.

4-3-1 Longitudinal Maneuver Identification

Data Acquisition The data used in parameter identification is generated by Simulink and CarSim co-simulation. In longitudinal maneuver, the steering angle is set to zero, which means the vehicle runs in a straight line, and the lateral velocity and yaw rate are also zero. Then the vehicle should be driven in a straight line with changing longitudinal velocity. For

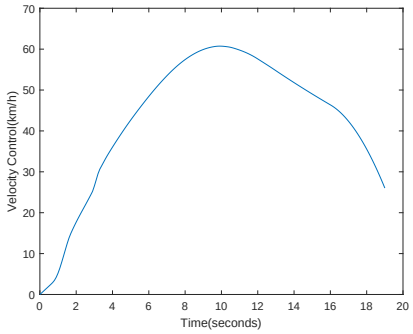

Figure 4-1: Driving Sample 1 for longitudinal maneuver

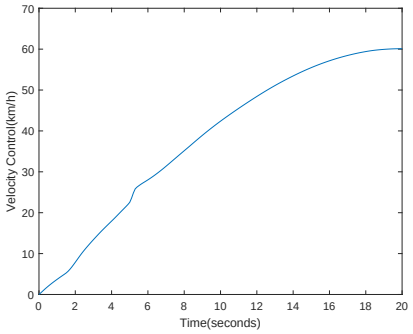

Figure 4-2: Driving Sample 2 for longitudinal maneuver

each section, two sets of data for different driving samples are given, showing in Fig. 4-1 and Fig. 4-2.
The test samples are selected as follows, Sample 1 includes the accelerating and decelerating process, and Sample 2 is a pure accelerating process.
The data obtained from CarSim is listed in Table 4-3.

Name	Longitudinal Velocity(m/s)	Wheel Spinning Velocity
Symbol	u	ωr_{wheel}

Table 4-3: Data obtained from CarSim for longitudinal maneuver

Parameter Identification According to Chapter 2, take eq. 2-10 into eq. 2-11, the vehicle longitudinal acceleration can be calculated as:

$$\dot{u} = 1/m \ (2C_{\lambda f}\lambda_f + 2C_{\lambda r}\lambda_r - F_{air}) \tag{4-10}$$

where the longitudinal slip ratio λ can be calculated by eq. 2-3. Then the parameters need to be identified are shown in Table 4-4. This vehicle is front-wheel driven and the slip ratio

Name	Symbol
Front Wheel Longitudinal Stiffness	$C_{\lambda f}$
Air Friction Coefficient	C_{air}

Table 4-4: Parameters need to be identified for bicycle model in longitudinal maneuver

for rear wheel is too small to get an accurate identification result, therefore, the rear wheel's longitudinal stiffness coefficient is set equal as the front one, which is $C_{\lambda r} = C_{\lambda f}$.
Then the estimated longitudinal velocity can be calculated by:

$$\tilde{u} = \dot{u}\Delta t \tag{4-11}$$

A set of data points can be derived as: $(u_1, \tilde{u}_1), (u_2, \tilde{u}_2), \ldots, (u_n, \tilde{u}_n)$.
The stiffness coefficient and air friction coefficient can be calculated as:

$$\min_{C_{\lambda f}, C_{air}} \parallel \mathbf{e_u} \parallel_2 = \min_{C_{\lambda f}, C_{air}} \parallel \mathbf{u} - \tilde{\mathbf{u}} \parallel_2 \tag{4-12}$$

This optimization problem can be solved by Interior-point method and the result is shown in Table 4-5.

Sample 1 Identification		Sample 2 Identification	
Parameter	Value	Parameter	Value
C_λ	50929	C_λ	76889
C_{air}	0.6246	C_{air}	0.3096

Table 4-5: Longitudinal maneuver identification result for bicycle model

Validation To prove the validity of the identified parameters, validation is required. The validation data is also generated from CarSim similar as **Data Acquisition**. Validation is also divided into parameter validation and system validation. Parameter validation validates each identified parameter, using longitudinal and lateral force measurements. System validation validates the vehicle as a whole and observe the difference between the estimated value and the true value of the vehicle system in longitudinal, lateral velocity and yaw rate.
To numerically display the validation result, Root Mean Square Error (RMSE) and variance accounted for (VAF) are used. And the validation plot are also presented. The validation result is shown in Table 4-6

Sample 1 Validation					Sample 2 Validation				
Term	Value	RMSE	VAF(%)	Fig.	Term	Value	RMSE	VAF(%)	Fig.
C_λ	50929	258.79	90.8	4-3	C_λ	76889	141.11	97.3	4-4
C_{air}	0.6246	39.45	22.1	4-5	C_{air}	0.3096	3.67	99.5	4-6
System Identification: u		0.8920	99.4	4-7	System Identification: u		0.9262	99.3	4-8

Table 4-6: Longitudinal maneuver validation result for bicycle model

Analysis In system validation for u, the VAF of both samples are very close, and over 99%, which means the estimated system perfectly imitate the real one in most sections. However, from 7 s to 10 s in Fig. 4-7 and Fig. 4-8, there is a rapid increase in velocity and a significant deviation in the prediction of velocity. This is because the slip ratio at this section is very high, where the force changes with a low speed with the change of the slip ratio, but the linear tire model ignores this section. Therefore, the linear tire model can predict very well at small acceleration changes, but the prediction of the linear tire model is not accurate at large slip ratio cases.
In parameter validation for C_λ and C_{air}, high errors occur in Sample 1 validation. Compared with Sample 2, the data of Sample 1 in longitudinal identification of bicycle model is an unsuitable data set. The value of each parameter should be well-identified with a suitable data set.
F_{air} is a small value comparing with F_x, but both forces affect the longitudinal movement together. The identification accuracy is higher when the parameter has the dominant effect

and vice versa. According to 2-12, air friction increase with the increase of velocity. So when the velocity is higher, the air resistance is also higher, and the influence of the air resistance on the longitudinal velocity is also greater. Therefore, the time spent in the high-speed stage of Sample 2 is longer; thus, the identification of C_{air} is more accurate.
In the following experiments, the results of the two samples are compared in other aspects.

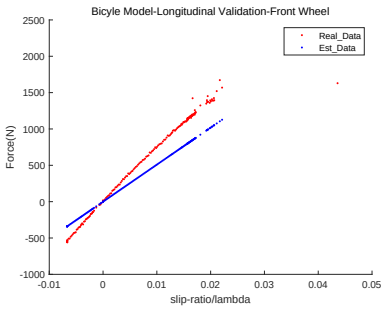

Figure 4-3: Driving Sample 1: Validation of C_λ for bicycle model

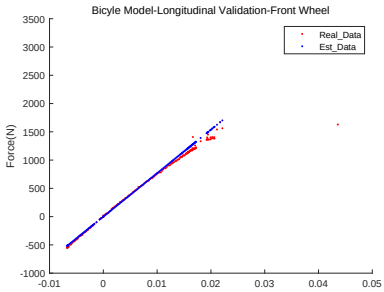

Figure 4-4: Driving Sample 2: Validation of C_λ for bicycle model

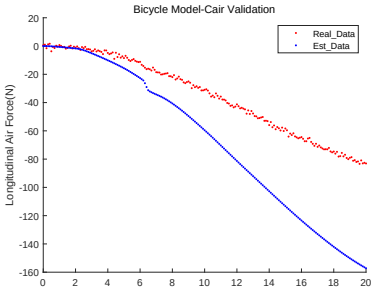

Figure 4-5: Driving Sample 1: Validation of C_{air} for bicycle model

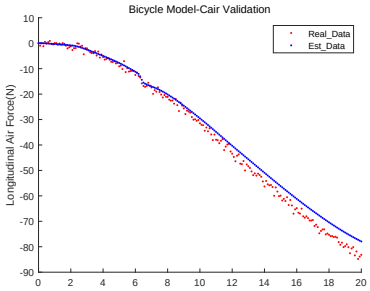

Figure 4-6: Driving Sample 2: Validation of C_{air} for bicycle model

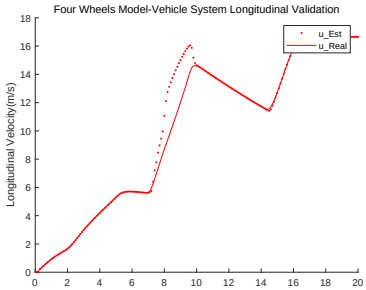

Figure 4-7: Driving Sample 1: System Validation of u for bicycle model

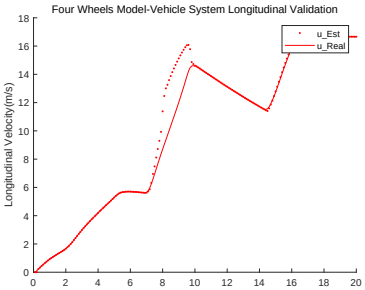

Figure 4-8: Driving Sample 2: System Validation of u for bicycle model

4-3-2 Lateral Maneuver Identification

Data Acquisition In lateral maneuver, the longitudinal velocity is controlled as $50km/h$ and the steering angle changes. Then the vehicle should be driven in a curve with constant velocity. Two sets of data for different driving sample are given, showing in Fig. 4-9 and Fig. 4-10.

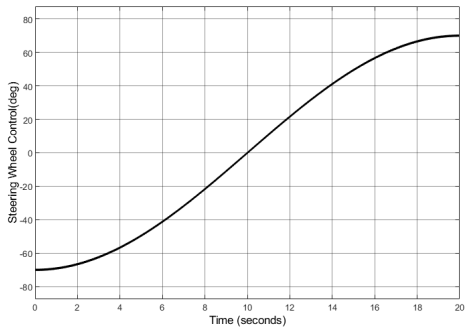

Figure 4-9: Driving Sample 1 for lateral maneuver

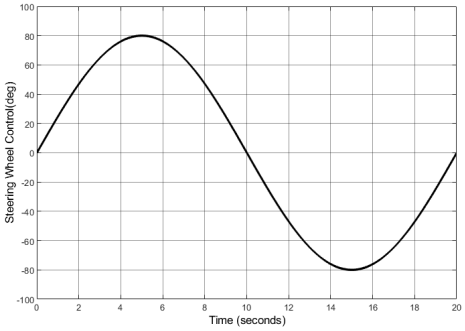

Figure 4-10: Driving Sample 2 for lateral maneuver

The data obtained from CarSim is listed in Table 4-7

Name	Symbol
Longitudinal Velocity(m/s)	u
Lateral Velocity(m/s)	v
Yaw Rate(rad/s)	r
Steering Angle(deg)	δ
Wheel Spinning Velocity(m/s)	ωr_{wheel}

Table 4-7: Data obtained from CarSim for lateral maneuver

Parameter Identification According to Chapter 2, take eq. 2-10 into eq. 2-11, the vehicle lateral acceleration and yaw rate can be calculated as:

$$\begin{aligned} \dot{v} &= 1/m(F_{yf} + F_{yr}) - ur \\ \dot{r} &= 1/I_z(l_f F_{yf} - l_r F_{yr}) \end{aligned} \tag{4-13}$$

Then the parameters need to be identified are shown in Table 4-8. with eq. 2-10, eq. 2-13, and eq. 2-14, the above equation can be rewritten in a state space equation:

$$\begin{bmatrix} \dot{v} \\ \dot{r} \end{bmatrix} = \begin{bmatrix} -\frac{C_{\alpha f}+C_{\alpha r}}{mu} & \frac{-l_f C_{\alpha f}+l_r C_{\alpha r}}{mu} - u \\ \frac{-l_f C_{\alpha f}+l_r C_{\alpha r}}{I_z u} & -\frac{l_f^2 C_{\alpha f}+l_r^2 C_{\alpha r}}{I_z u} \end{bmatrix} \begin{bmatrix} v \\ r \end{bmatrix} + \begin{bmatrix} \frac{C_{\alpha f}}{m} \\ \frac{l_f C_{\alpha f}}{I_z} \end{bmatrix} \delta \tag{4-14}$$

Then the parameters need to be identified are shown in Table 4-8.

Name	Symbol
Front Wheel Lateral Stiffness	$C_{\alpha f}$
Rear Wheel Lateral Stiffness	$C_{\alpha r}$
Yaw Inertia	I_z

Table 4-8: Parameters need to be identified for bicycle model in lateral maneuver

Similar to the longitudinal identification, the estimated lateral velocity and yaw rate can be calculated by:

$$\begin{aligned} \tilde{v} &= \dot{v}\Delta t \\ \tilde{r} &= \dot{r}\Delta t \end{aligned} \tag{4-15}$$

A set of data points can be derived as: $(\begin{bmatrix} v_1 \\ r_1 \end{bmatrix}, \begin{bmatrix} \tilde{v}_1 \\ \tilde{r}_1 \end{bmatrix}), (\begin{bmatrix} v_2 \\ r_2 \end{bmatrix}, \begin{bmatrix} \tilde{v}_2 \\ \tilde{r}_2 \end{bmatrix}), \ldots, (\begin{bmatrix} v_n \\ r_n \end{bmatrix}, \begin{bmatrix} \tilde{v}_n \\ \tilde{r}_n \end{bmatrix})$.
The lateral stiffness of front and rear wheel and the yaw inertia can be calculated by solving the following optimization problem by Interior-point method:

$$\min_{C_{\alpha f}, C_{\alpha r}, I_z} \parallel \mathbf{e}_{\mathbf{v},\mathbf{r}} \parallel_2 = \min_{C_{\alpha f}, C_{\alpha r}, I_z} \parallel \begin{bmatrix} \mathbf{v} \\ \mathbf{r} \end{bmatrix} - \begin{bmatrix} \tilde{\mathbf{v}} \\ \tilde{\mathbf{r}} \end{bmatrix} \parallel_2 \tag{4-16}$$

The result is shown in Table 4-9

Parameter	$C_{\alpha f}$	$C_{\alpha r}$	I_z
Sample 1	28143	50398	5000
Sample 2	46341	21663	1697

Table 4-9: Lateral maneuver identification result for bicycle model

Validation The real lateral force compares with estimated lateral force for front and real wheels calculated from eq. 2-10 to validate $C_{\alpha f}$ and $C_{\alpha r}$ and uses yaw rate to validate I_z. The estimation of lateral velocity v and yaw rate r are used for lateral maneuver system validation The validation result is shown in Table 4-10

Analysis In system validation for v, the result for Sample 2 is better than Sample 1, and for r, the result for Sample 1 is better than Sample 2. Similar to longitudinal maneuver validation, the parameter identification result for Sample 2 is significantly better than Sample 1. So it can be inferred that in Sample 1, parameter coupling occurs between the parameters C_α and I_z. The estimated forces calculated from C_α create a large error with the real value and produces excessive torque. However, the same excessive moment of inertia 'weakens' the effect of excessive torque and makes the system's overall performance normal. One way to solve this problem is to let the data sets have persistency of excitation [25]. Persistency of excitation of an input or a noise signal is of importance in system identification, and adaptive control [26]. In system identification, it can be understood that when the data set is in sufficient

Sample 1 Validation					Sample 2 Validation				
Term	Value	RMSE	VAF(%)	Fig.	Term	Value	RMSE	VAF(%)	Fig.
$C_{\alpha f}$	28143	228.62	88.9	4-11	$C_{\alpha f}$	46341	71.94	98.9	4-12
$C_{\alpha r}$	50398	212.81	75.9	4-13	$C_{\alpha r}$	21663	156.26	87.0	4-14
I_z	5000	0.0448	58.6	4-15	I_z	1697	0.0059	99.3	4-16
System Identification: v		0.0059	85.3	4-17	System Identification: v		0.0047	90.7	4-18
System Identification: r		0.0259	98.3	4-17	System Identification: r		0.0746	85.7	4-18

Table 4-10: Lateral maneuver validation result for bicycle model

conditions, the parameters identified are more likely to converge. A sufficient data set can be expressed as multi-frequency oscillations. Sample 2 is a sinusoidal curve, so it is more sufficient than Sample 1, and the parameter is closer to the real value.
In this model, the influence of longitudinal force on the yaw rate is ignored because the longitudinal force is smaller than the lateral force, so the influence of torque generated by longitudinal force is relatively small. In the case of low requirements for model identification accuracy, such a linear model can be used to reduce the complexity and calculation, but at the same time, some errors may be hard to prevent.

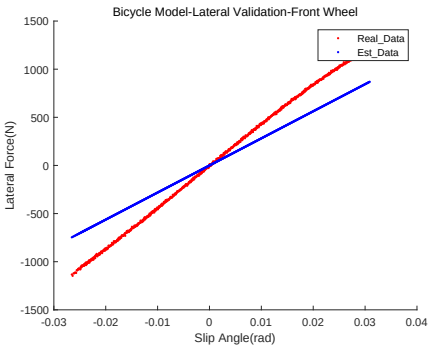

Figure 4-11: Driving Sample 1: Validation of $C_{\alpha f}$ for bicycle model

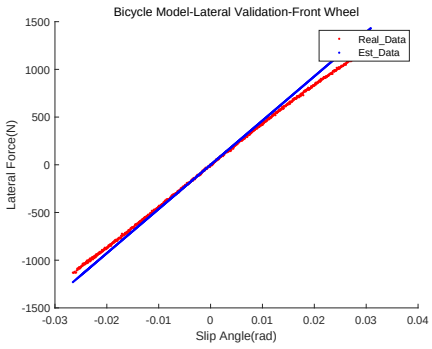

Figure 4-12: Driving Sample 2: Validation of $C_{\alpha f}$ for bicycle model

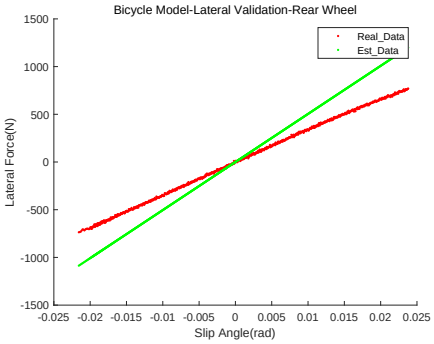

Figure 4-13: Driving Sample 1: Validation of $C_{\alpha r}$ for bicycle model

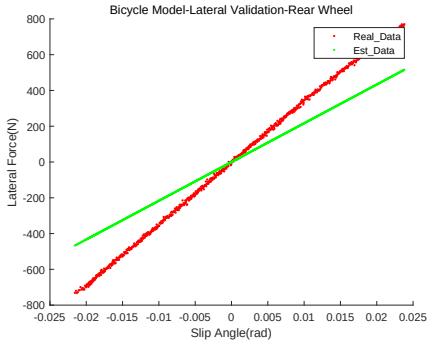

Figure 4-14: Driving Sample 2: Validation of $C_{\alpha r}$ for bicycle model

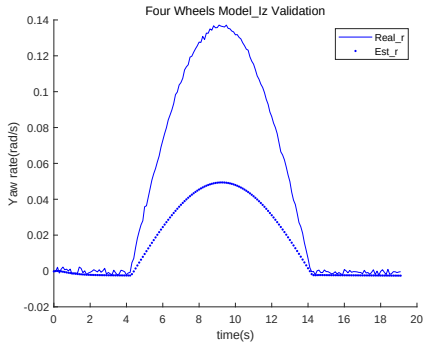

Figure 4-15: Driving Sample 1: Validation of I_z for bicycle model

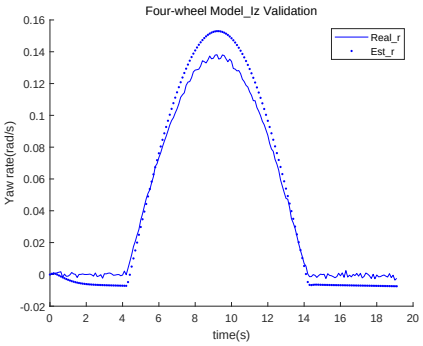

Figure 4-16: Driving Sample 2: Validation of I_z for bicycle model

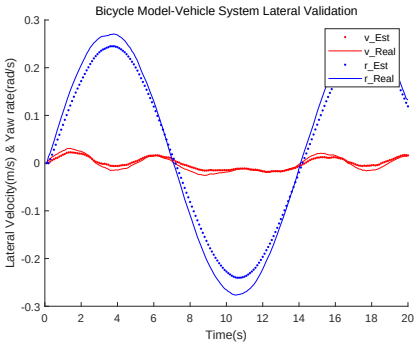

Figure 4-17: Driving Sample 1: System Validation of v and r for bicycle model

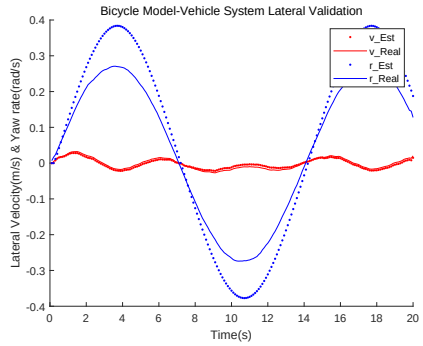

Figure 4-18: Driving Sample 2: System Validation of v and r for bicycle model

4-4 Four Wheels Model Identification

The bicycle model is linearized and simplified in many places, and the yaw acceleration is calculated without considering the influence of the vehicle's longitudinal force, which causes errors. Theoretically, these errors are endurable when the system accuracy is not required to be high. Still, if the system accuracy is needed to be high, there is a certain possibility that the identification accuracy does not meet the requirements.
Therefore, in this section, Interior-point algorithm is used to identify four wheels vehicle and the Dugoff model is used as the tire model.

4-4-1 Longitudinal Maneuver Identification

Data Acquisition The data sets used for identification and validation are the same as those in bicycle model.

Parameter Identification According to eq. 2-15, the vehicle longitudinal acceleration can be calculated as:

$$\dot{u} = 1/m \ (F_{xfl} + F_{xfr} + F_{xrl} + F_{xrr} - F_{air}) \tag{4-17}$$

Then the parameters need to be identified are shown in Table 4-11.

Name	Symbol
Front Left Wheel Longitudinal Stiffness	$C_{\lambda fl}$
Front Right Wheel Longitudinal Stiffness	$C_{\lambda fr}$
Friction Coefficient	μ
Air Friction Coefficient	C_{air}

Table 4-11: Parameters need to be identified for four wheels model in longitudinal maneuver

This vehicle is front-wheel driven and the slip ratio for rear wheel is too small to show a pattern, therefore, the rear wheels' longitudinal stiffness coefficients are set equal as the front, which are $C_{\lambda rl} = C_{\lambda fl}$ and $C_{\lambda rr} = C_{\lambda fr}$.
Then the estimated longitudinal velocity can be calculated by eq. 4-11 and a set of data points can be derived as: $(u_1, \tilde{u}_1), (u_2, \tilde{u}_2), \ldots, (u_n, \tilde{u}_n)$.
The stiffness coefficient and air friction coefficient can be calculated as:

$$\min_{C_{\lambda fl}, C_{\lambda fr}, \mu, C_{air}} \parallel \mathbf{e_u} \parallel_2 = \min_{C_{\lambda fl}, C_{\lambda fr}, \mu, C_{air}} \parallel \mathbf{u} - \tilde{\mathbf{u}} \parallel_2 \tag{4-18}$$

The identification result is shown in Table 4-12.

Parameter	$C_{\lambda fl}$	$C_{\lambda fr}$	μ	C_{air}
Sample 1	62514	78890	0.9390	0.4798
Sample 2	80976	80391	0.5036	0.3843

Table 4-12: Longitudinal maneuver identification result for four wheels model

Validation The validation result is shown in Table 4-13

Sample 1 Validation					Sample 2 Validation				
Term	Value	RMSE	VAF(%)	Fig.	Term	Value	RMSE	VAF(%)	Fig.
$C_{\lambda fl}$	62514	142.89	97.2	4-19	$C_{\lambda fl}$	80976	52.99	99.6	4-20
$C_{\lambda fr}$	78890	103.60	98.5	4-21	$C_{\lambda fr}$	80391	49.65	99.7	4-22
μ	0.939				μ	0.5036			
C_{air}	0.4798	19.92	80.1	4-23	C_{air}	0.3843	7.25	97.4	4-24
System Identification: u		0.1662	100	4-25	System Identification: u		0.1170	100	4-26

Table 4-13: Longitudinal maneuver validation result for four wheels model

Analysis Compared with the bicycle model, the four wheels model considers the force of the left wheel and the right wheel of the vehicle, respectively. In addition to considering the longitudinal motion, it is also necessary to maintain the torque balance to make the vehicle move in a straight line. More relational constraints can also avoid the occurrence of parameter coupling and increase the accuracy of identification. For example, in Sample 1, the results of the four wheels model validation were significantly improved. The four wheels model system validation results of Sample 2 are very close to that of Sample 1, both with minimal errors. Therefore, in system identification, models with high accuracy are more likely to identify better results for different data sets, but it also causes more computational load. For vehicle longitudinal identification, the calculation time of the four wheels model is about 20 s, although this is longer than the experiment for the bicycle model about 8 s, the time consumption is still acceptable. Therefore, four wheels model is suitable for vehicle identification and control.

It can also be seen from the system identification results of u that at the high acceleration stage between 7 s and 10 s, the estimation error of the Dugoff tire model is tiny, VAF is close to 100%. The Dugoff model can simulate the saturation state between tire force and slip ratio, whereas the linear model is incapable in this range.

μ is the friction coefficient, which calculates the tire force together with the stiffness coefficient C_λ. In general, the accuracy of Sample 2 is higher, so the identified parameters result of Sample 2 are selected for lateral maneuver identification.

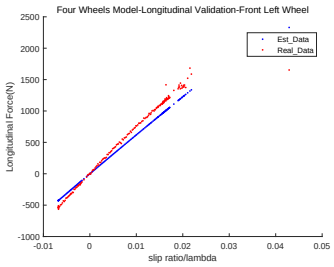

Figure 4-19: Driving Sample 1: Validation of $C_{\lambda f}$ for four wheels model

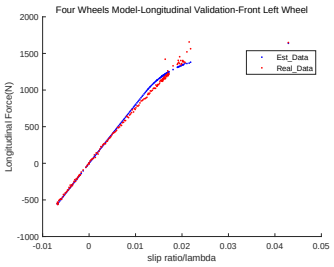

Figure 4-20: Driving Sample 2: Validation of $C_{\lambda f}$ for four wheels model

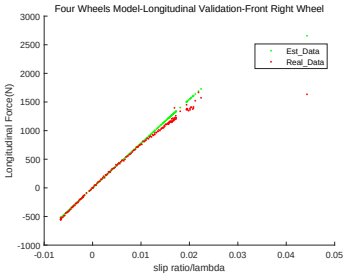

Figure 4-21: Driving Sample 1: Validation of $C_{\lambda r}$ for four wheels model

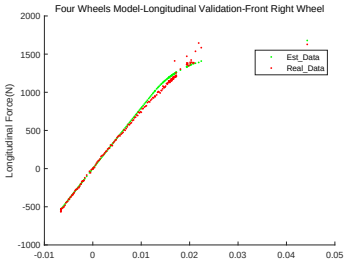

Figure 4-22: Driving Sample 2: Validation of $C_{\lambda r}$ for four wheels model

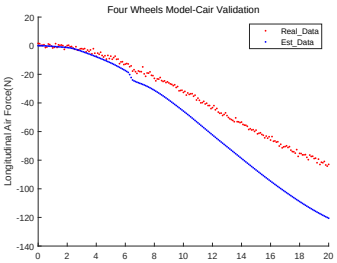

Figure 4-23: Driving Sample 1: Validation of C_{air} for four wheels model

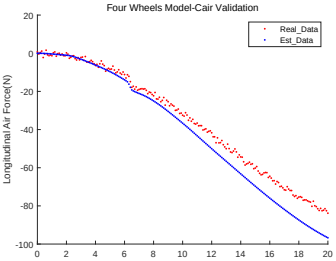

Figure 4-24: Driving Sample 2: Validation of C_{air} for four wheels model

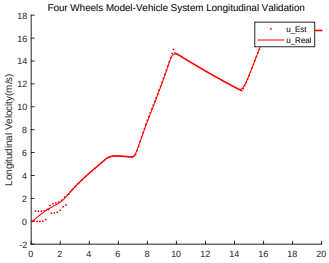

Figure 4-25: Driving Sample 1: System Validation of u for four wheels model

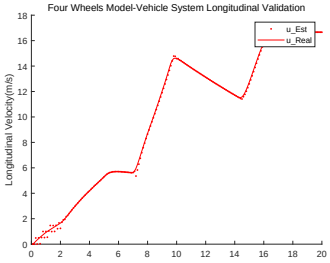

Figure 4-26: Driving Sample 2: System Validation of u for four wheels model

4-4-2 Lateral Maneuver Identification

Data Acquisition The data sets used for identification and validation are the same as those in bicycle model.

Parameter Identification According to eq. 2-15, the vehicle lateral acceleration and yaw rate can be calculated as:

$$\begin{aligned}\dot{v} &= 1/m(F_{yfl} + F_{yfr} + F_{yrl} + F_{yrr}) - ur \\ \dot{r} &= 1/I_z(l_f(F_{yfl} + F_{yfr}) - l_r(F_{yrl} + F_{yrr}) - B_l(F_{xfl} + F_{xrl}) + B_r(F_{xfr} + F_{xrr}))\end{aligned} \tag{4-19}$$

Then the parameters need to be identified are shown in Table 4-14.

Name	Symbol
Front Left Wheel Lateral Stiffness	$C_{\alpha fl}$
Front Right Wheel Lateral Stiffness	$C_{\alpha fr}$
Rear Left Wheel Lateral Stiffness	$C_{\alpha rl}$
Rear Right Wheel Lateral Stiffness	$C_{\alpha rr}$
Yaw Inertia	I_z

Table 4-14: Parameters need to be identified for four wheels model in lateral maneuver

The estimated lateral velocity and yaw rate can be calculated by eq. 4-15 and a set of data points can be derived as: $(\begin{bmatrix} v_1 \\ r_1 \end{bmatrix}, \begin{bmatrix} \tilde{v}_1 \\ \tilde{r}_1 \end{bmatrix}), (\begin{bmatrix} v_2 \\ r_2 \end{bmatrix}, \begin{bmatrix} \tilde{v}_2 \\ \tilde{r}_2 \end{bmatrix}), \ldots, (\begin{bmatrix} v_n \\ r_n \end{bmatrix}, \begin{bmatrix} \tilde{v}_n \\ \tilde{r}_n \end{bmatrix})$.

The lateral stiffness of four wheels and the yaw inertia can be calculated by solving the following optimization problem by Interior-point method:

$$\min_{C_{\alpha i}, I_z} \parallel \mathbf{e}_{\mathbf{v},\mathbf{r}} \parallel_2 = \min_{C_{\alpha i}, I_z} \parallel \begin{bmatrix} \mathbf{v} \\ \mathbf{r} \end{bmatrix} - \begin{bmatrix} \tilde{\mathbf{v}} \\ \tilde{\mathbf{r}} \end{bmatrix} \parallel_2,\ i = fl, fr, rl, rr \tag{4-20}$$

The result is shown in Table 4-15

Parameter	$C_{\alpha fl}$	$C_{\alpha fr}$	$C_{\alpha rl}$	$C_{\alpha rr}$	I_z
Sample 1	44021	39093	50148	31825	1767
Sample 2	47254	39950	40064	37433	1810

Table 4-15: Lateral maneuver identification result for four wheels model

Validation The validation result is shown in Table 4-16

Sample 1 Validation					Sample 2 Validation				
Term	Value	RMSE	VAF(%)	Fig.	Term	Value	RMSE	VAF(%)	Fig.
$C_{\alpha fl}$	44021	38.83	99.7	4-27	$C_{\alpha fl}$	47254	62.08	99.2	4-28
$C_{\alpha fr}$	39093	78.33	98.8	4-29	$C_{\alpha fr}$	39950	66.97	99.1	4-30
$C_{\alpha rl}$	50148	173.44	84.5	4-31	$C_{\alpha rl}$	40064	85.58	96.2	4-32
$C_{\alpha rr}$	31825	59.72	98.2	4-33	$C_{\alpha rr}$	37433	54.10	98.6	4-34
I_z	1767	0.0053	99.4	4-35	I_z	1810	0.0038	99.7	4-36
System Identification: v		0.089	65.6	4-37	System Identification: v		0.0044	92	4-38
System Identification: r		0.0242	98.5	4-37	System Identification: r		0.0197	99	4-38

Table 4-16: Lateral maneuver validation result for four wheels model

Analysis It can be seen from the parameter validation results that the accuracy of the four wheels model is significantly improved compared with the bicycle model. Sample 2 VAF has been raised above 99%. Although the error in Sample 1 in $C_{\alpha rl}$ is still large, it still has a significant improvement over the bicycle model. It can be seen that the parameters are more likely to converge to the real value in a relatively accurate model. The identification time was about 36 seconds on the computer used in this thesis, while the bicycle model took about 13 seconds. Although the running time is three times longer, it is still within the acceptable range.

It can also be seen from the parameter validation that the Dugoff model lacks a peak value between the linear section and the saturation section compared with the actual tire model. However, as shown in the system identification of Sample 2 that the error in this section has a relatively small impact on the whole system. The Magic Formula accurately describes the real-time model. With more than 30 parameters per tire, the Interior-point method is challenging to directly optimize such a high dimensional model. In section 5-3-1, the Magic Formula model is attempted to identify by using GA.

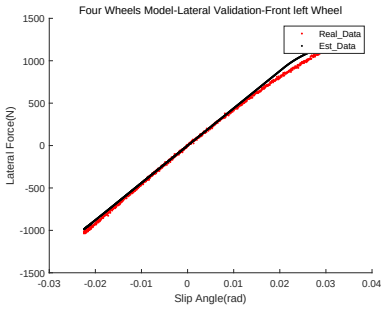

Figure 4-27: Driving Sample 1: Validation of $C_{\alpha fl}$ for four wheels model

Figure 4-28: Driving Sample 2: Validation of $C_{\alpha fl}$ for four wheels model

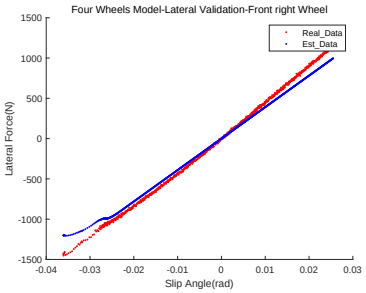

Figure 4-29: Driving Sample 1: Validation of $C_{\alpha fr}$ for four wheels model

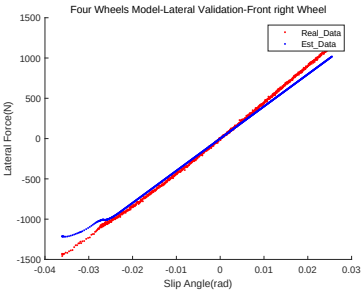

Figure 4-30: Driving Sample 2: Validation of $C_{\alpha fr}$ for four wheels model

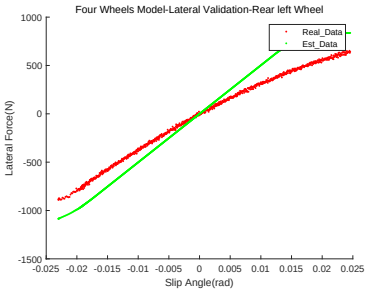

Figure 4-31: Driving Sample 1: Validation of $C_{\alpha rl}$ for four wheels model

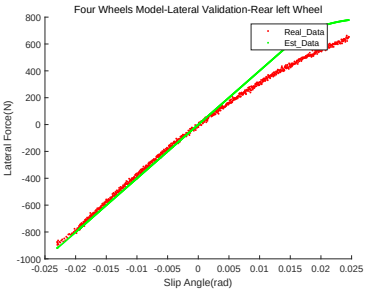

Figure 4-32: Driving Sample 2: Validation of $C_{\alpha rl}$ for four wheels model

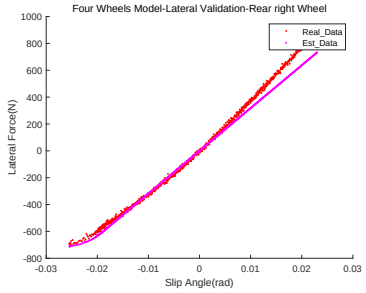

Figure 4-33: Driving Sample 1: Validation of $C_{\alpha rr}$ for four wheels model

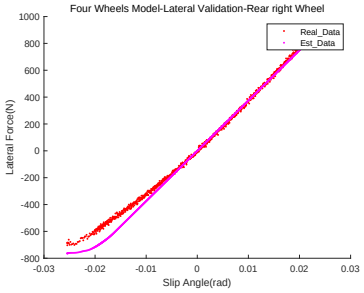

Figure 4-34: Driving Sample 2: Validation of $C_{\alpha rr}$ for four wheels model

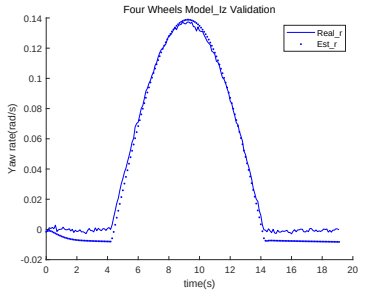

Figure 4-35: Driving Sample 1: Validation of I_z for four wheels model

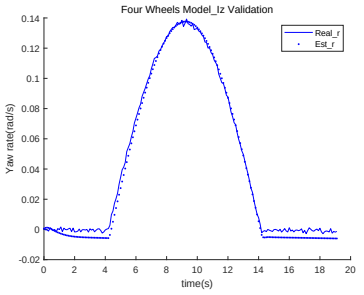

Figure 4-36: Driving Sample 2: Validation of I_z for four wheels model

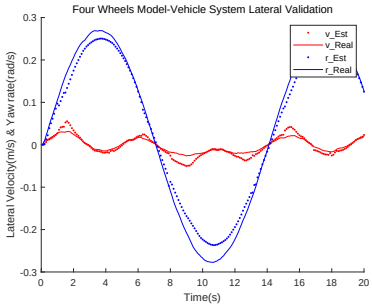

Figure 4-37: Driving Sample 1: System Validation of v and r for four wheels model

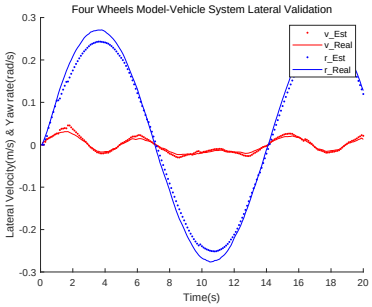

Figure 4-38: Driving Sample 2: System Validation of v and r for four wheels model

4-5 Conclusion

This chapter introduces the system identification of the bicycle model and four wheels model by using the Interior-point method. The bicycle model is linearized and ignoring the influence of the vehicle's width. The tire model also adopts the simplified tire model. The identification of the four wheels model takes into account the influence of longitudinal force on the yaw movement and the difference of vertical force on the left and right side caused by roll movement, and also adopts a more complex Dugoff tire model.
Validation results show that the overall result of RMSE and VAF of the four wheels model is better than that of the bicycle model, so the accuracy has been greatly improved. There are two main reasons for this.
First, the mathematics model is more accurate. For example, in the calculation of yaw motion, although the influence of longitudinal force is smaller than that of lateral force, the influence will become larger as time accumulates.
The second is that in each identification model, the number of equations is smaller than the number of unknown parameters, so it is possible that there will be coupling between the parameters, such as C_λ and C_{air}, C_α and I_z. In more complex models, each parameter establishes more relationships with the system, limiting the size of the parameter and distinguishing it from other parameters. This makes the parameters more likely to converge to the real value.
The above experiments also compared the influence of different data sets on the final identification results. For a good data set, good system validation results are needed and good validation results for each parameter are also required. Better data sets require selection through identification results. The data set should also have persistency of excitation, which eases the coupling between parameters and improve the parameters convergency.

Chapter 5

Vehicle Identification by Other Algorithms

In addition to the Interior-point method, many other algorithms can also be used as system identification algorithms. In this study, Unscented Kalman Filter (UKF) will also be practiced and compared with the Interior-point method to analyze the advantages and disadvantages of each method and its application scenarios. For the problem of UKF, Particle Swarm Optimization-Unscented Kalman Filter (PSO-UKF) will also be tried to optimize UKF to explore if this algorithm is practical.
Two tire models were introduced in Section 2-1, and the Dugoff model has fewer parameters but is less precise than the Magic Formula. However, the Magic Formula has ten times as many parameters as the Dugoff model, which the identification method previously attempted would be challenging to optimize on this dimension. Genetic Algorithm (GA) is a relatively effective algorithm in the identification of the Magic Formula. Although the final result is not satisfactory, GA identification of the Magic Formula is still presented and analyzed as a failure control group in this project.

5-1 Unscented Kalman Filter Identification

5-1-1 UKF Introduction

Kalman Filter (KF) is an algorithm that uses the linear system state equations to optimally estimate the state of a dynamic system through input and output observations. When using KF to do system identification, unknown parameters are estimated with the state parameters. Since the observation data includes the influence of random perturbations and interference in the system, the optimal estimation can also be regarded as a filtering process [4] [27].
UKF has become a popular technique in nonlinear estimation which include estimating the state of a nonlinear dynamic system and the parameters for nonlinear system identification [28]. The following sections will introduce UKF and how to use UKF on an identification problem.

5-1-2 UKF

The UKF approximates the nonlinear transformation through a set of sample points. These sample points are chosen by Unscented Transformation(UT), which calculates the statistics of a random variable which undergoes a nonlinear transformation [29].
Assume x has mean $\overline{x}$ and covariance P_x. To calculate the statistics of y, a matrix χ of $2L+1$ sigma vectors χ_i is constructed where L is the dimension of x. W_i is the corresponding weight value as the following [28].

$$\begin{aligned}
\lambda &= \alpha^2(L+\kappa) - L \\
\chi_0 &= \overline{x} \\
\chi_i &= \overline{x} + (\sqrt{(L+\lambda)P_x})_i \qquad i = 1, \ldots, L \\
\chi_i &= \overline{x} - (\sqrt{(L+\lambda)P_x})_{i-L} \quad i = L+1, \ldots, 2L \\
W_0^{(m)} &= \frac{\lambda}{L+\lambda} \\
W_0^{(c)} &= \frac{\lambda}{L+\lambda} + (1 - \alpha^2 + \beta) \\
W_i^{(m)} &= W_i^{(c)} = \frac{1}{2(L+\lambda)} \qquad i = 1, \ldots, 2L
\end{aligned} \tag{5-1}$$

In the above equations, λ is the principal scaling parameter. α determines the spread of sigma points about the mean $\hat{x}$ and be set as 0.01. The constant κ is a secondary scaling parameter, generally set to $3 - L$. In here, κ is set as 0. The constant β is used to incorporate prior knowledge of the distribution and $\beta = 2$ is optimal for Gaussian distributions [29]. Then the UKF algorithm can be written as following equations.
Calculate the sigma points:

$$\chi(k-1) = [\hat{x}(k-1)\ \hat{x}(k-1) \pm \sqrt{(L+\lambda)P(k-1)}] \tag{5-2}$$

Time update:

$$\begin{aligned}
\chi(k|k-1) &= f(\chi(k-1)) \\
\hat{x}(k|k-1) &= \sum_{i=0}^{2L} W_i^{(m)} \chi_i(k|k-1) \\
P(k|k-1) &= \sum_{i=0}^{2L} W_i^{(c)} [\chi_i(k|k-1) - \hat{x}(k|k-1)][\chi_i(k|k-1) - \hat{x}(k|k-1)]^T + Q \\
Y(k|k-1) &= h(\chi(k|k-1)) \\
\hat{y}(k|k-1) &= \sum_{i=0}^{2L} W_i^{(m)} Y_i(k|k-1)
\end{aligned} \tag{5-3}$$

Update after the measurement of y(k):

$$\begin{aligned} P_{y(k),y(k)} &= \sum_{i=0}^{2L} W_i^{(c)}[Y_i(k|k-1) - \hat{y}(k|k-1)][Y_i(k|k-1) - \hat{y}(k|k-1)]^T + R \\ P_{x(k),y(k)} &= \sum_{i=0}^{2L} W_i^{(c)}[\chi_i(k|k-1) - \hat{x}(k|k-1)][Y_i(k|k-1) - \hat{y}(k|k-1)]^T \\ K &= P_{x(k),y(k)} P_{y(k),y(k)}^{-1} \\ \hat{x}(k) &= \hat{x}(k|k-1) + K(y(k) - \hat{y}(k|k-1)) \\ P(k) &= P(k|k-1) - K(P_{y(k),y(k)})K^T \end{aligned} \tag{5-4}$$

5-1-3 Identification by UKF

The UKF has been introduced, how to identify the parameters of a system will be given in this section.
The UKF approaches to determine the unknown parameter is obtained by extending the state vector x with the parameter vector θ [30]. The dynamic model and measurements can be put in the following form:

$$\begin{aligned} x(k+1) &= f(x(k), \theta) + w(k) \\ y(k) &= h(x(k), \theta) + v(k) \end{aligned} \tag{5-5}$$

The vector x and f have the following structure:

$$x(k) = \begin{bmatrix} s_1(k) \\ s_2(k) \\ \vdots \\ s_n(k) \\ -- \\ \theta_1 \\ \theta_2 \\ \vdots \\ \theta_m \end{bmatrix}; \quad f(k) = \begin{bmatrix} f_1(x(k), \theta) \\ f_2(x(k), \theta) \\ \vdots \\ f_n(x(k), \theta) \\ -- \\ \theta_1 \\ \theta_2 \\ \vdots \\ \theta_m \end{bmatrix} \tag{5-6}$$

where $s_i(k)$ indicates the states of the system and θ_j indicated the unknown parameters of the system. The parameters keep constant over time. Then the parameters can be identified with the state variables by UKF [31].
In the identification by using UKF, the identification and validation data are the same as the ones in Chapter 4 and only the four wheels vehicle model is identified.
Since UKF is updated with the value of each step, the variation of parameters in each step is relatively small, and the existing data length is not sufficient for the parameter states of UKF to converge to the optimal solution. Therefore, the same set of data is used for multiple times in a loop [31]. The final value of the parameter states of the previous group of iteration is set to the initial value of the parameter states of the next group of iteration. When the parameter state is no longer changing, this value can be taken as the parameter value estimated by UKF.

5-1-4 Longitudinal Maneuver Identification

Parameter Identification The state matrix in this experiment is constructed as:

$$x(k) = \begin{bmatrix} u(k) \\ r(k) \\ C_{\lambda l} \\ C_{\lambda r} \\ \mu \\ C_{air} \end{bmatrix} \tag{5-7}$$

$f(x(k), \theta)$ can be constructed according to eq. 2-15 and $h(x(k), \theta)$ takes the measurement value of u and r. The key problem of UKF is that its estimated performance is greatly affected by the values of the covariance matrices Q and R which are state noise and measurement noise matrices. According to KF, Q and R must take into account the randomness of the corresponding noises, however, as these are usually unknown [2]. For measurement and state noise matrices, they need to be tuned manually by trail and error [2]. This raises the question of what happens if the R and Q matrices of Sample 1 is applied to Sample 2, where the result is shown in the third row of Table 5-1.

After tuning, the measurement noise matrix R in longitudinal maneuver identification for Sample 1 is $\begin{bmatrix} 1 \times 10^{-5} & 0 \\ 0 & 1 \times 10^{-5} \end{bmatrix}$.

The state noise matrix Q is $\begin{bmatrix} 1 \times 10^{-4} & 0 & 0 & 0 & 0 & 0 \\ 0 & 1 \times 10^{-4} & 0 & 0 & 0 & 0 \\ 0 & 0 & 1 \times 10^{-4} & 0 & 0 & 0 \\ 0 & 0 & 0 & 1 \times 10^{-4} & 0 & 0 \\ 0 & 0 & 0 & 0 & 1 \times 10^{-4} & 0 \\ 0 & 0 & 0 & 0 & 0 & 1 \times 10^{-4} \end{bmatrix}$.

The measurement noise matrix R in longitudinal maneuver identification for Sample 2 is $\begin{bmatrix} 1 \times 10^{-6} & 0 \\ 0 & 1 \times 10^{-6} \end{bmatrix}$.

The state noise matrix Q is $\begin{bmatrix} 1 \times 10^{-3} & 0 & 0 & 0 & 0 & 0 \\ 0 & 1 \times 10^{-3} & 0 & 0 & 0 & 0 \\ 0 & 0 & 1 \times 10^{-3} & 0 & 0 & 0 \\ 0 & 0 & 0 & 1 \times 10^{-3} & 0 & 0 \\ 0 & 0 & 0 & 0 & 1 \times 10^{-3} & 0 \\ 0 & 0 & 0 & 0 & 0 & 1 \times 10^{-3} \end{bmatrix}$.

The result of identification by UKF is shown in Table 5-1.

Parameter	$C_{\lambda fl}$	$C_{\lambda fr}$	μ	C_{air}
Sample 1	77063	69472	0.2986	3.3496
Sample 2 with Sample 1 R and Q matrices	26559	27198	2.3921	-1.1315
Sample 2	68346	65507	0.5924	0.5477

Table 5-1: Longitudinal maneuver identification result for four wheels model

Validation The validation result is shown in Table 5-2 and Table 5-3 and also be quantitized by Root Mean Square Error (RMSE) and variance accounted for (VAF).

Sample 1 Validation					Sample 2 Validation				
Term	Value	RMSE	VAF(%)	Fig.	Term	Value	RMSE	VAF(%)	Fig.
$C_{\lambda fl}$	77063	220.58	93.3	5-1	$C_{\lambda fl}$	68346	76.64	99.2	5-2
$C_{\lambda fr}$	69472	231.60	92.6	5-3	$C_{\lambda fr}$	65507	102.7	98.5	5-4
μ	0.286				μ	0.5924			
C_{air}	3.3496	406.48	0	5-5	C_{air}	00.5477	29.23	57.0	5-6
System Identification: u		0.3181	99.9	5-7	System Identification: u		0.1093	100	5-8

Table 5-2: Longitudinal maneuver validation result for four wheels model in UKF identification

Sample 2 with Sample 1 R and Q matrices Validation				
Term	Value	RMSE	VAF(%)	Fig.
$C_{\lambda fl}$	26559	542.49	59.5	5-9
$C_{\lambda fr}$	27198	532.95	60.8	5-10
μ	2.3921			
C_{air}	-1.1315	390	0	5-11
System Identification: u		0.588	99.7	5-12

Table 5-3: Longitudinal maneuver Sample 2 validation result by using Sample 1 R and Q matrices in UKF identification

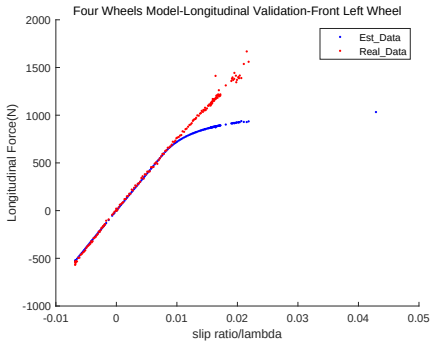

Figure 5-1: Driving Sample 1: Validation of $C_{\lambda f}$ for four wheels model in UKF identification

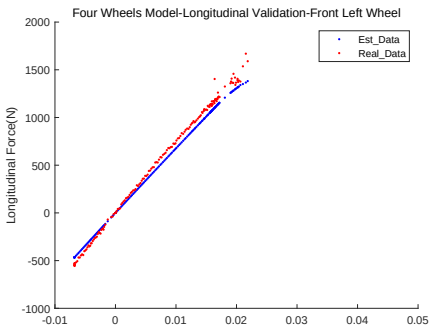

Figure 5-2: Driving Sample 2: Validation of $C_{\lambda f}$ for four wheels model in UKF identification

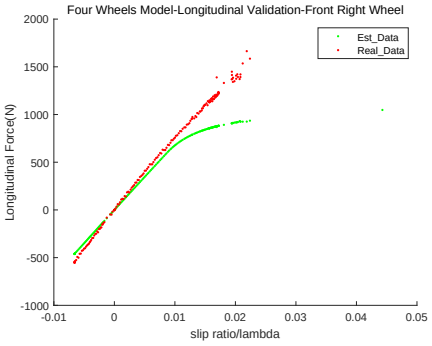

Figure 5-3: Driving Sample 1: Validation of $C_{\lambda r}$ for four wheels model in UKF identification

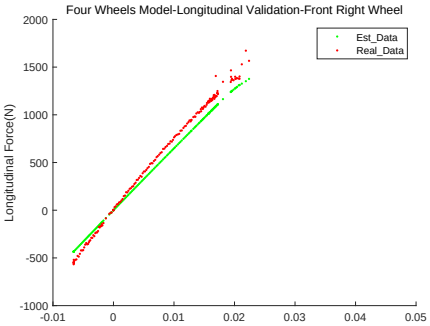

Figure 5-4: Driving Sample 2: Validation of $C_{\lambda r}$ for four wheels model in UKF identification

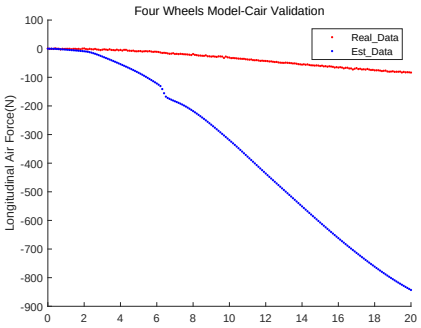

Figure 5-5: Driving Sample 1: Validation of C_{air} for four wheels model in UKF identification

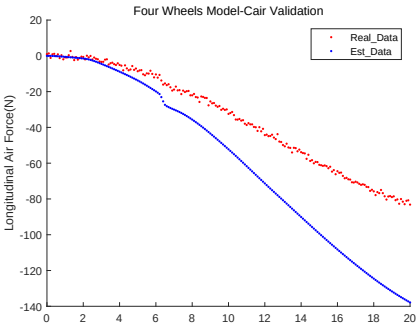

Figure 5-6: Driving Sample 2: Validation of C_{air} for four wheels model in UKF identification

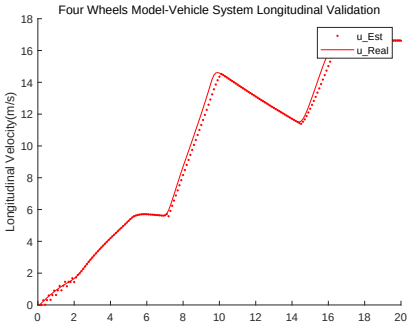

Figure 5-7: Driving Sample 1: System Validation of u for four wheels model in UKF identification

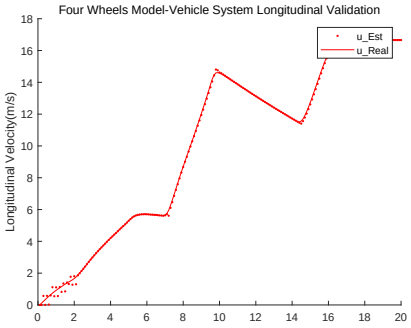

Figure 5-8: Driving Sample 2: System Validation of u for four wheels model in UKF identification

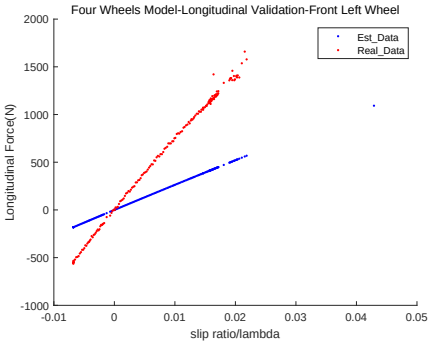

Figure 5-9: Driving Sample 2 with Sample 1 R and Q matrices: Validation of $C_{\lambda f}$ for four wheels model in UKF identification

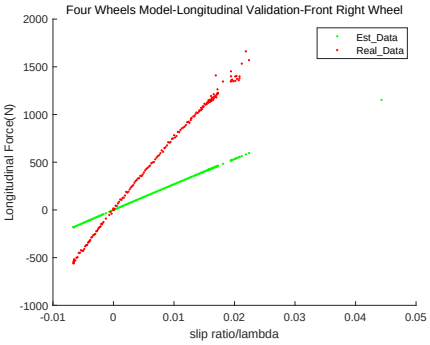

Figure 5-10: Driving Sample 2 with Sample 1 R and Q matrices: Validation of $C_{\lambda r}$ for four wheels model in UKF identification

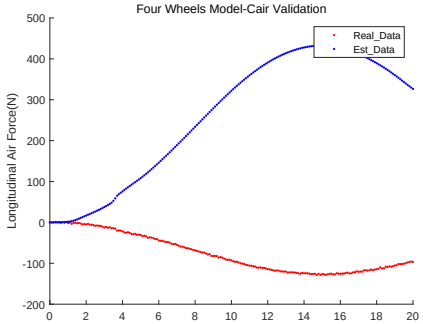

Figure 5-11: Driving Sample 2 with Sample 1 R and Q matrices: Validation of C_{air} for four wheels model in UKF identification

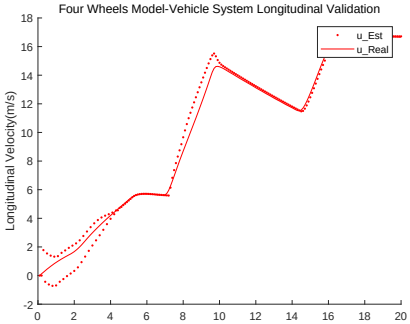

Figure 5-12: Driving Sample 2 with Sample 1 R and Q matrices: System Validation of u for four wheels model in UKF identification

5-1-5 Lateral Maneuver Identification

The state matrix in this experiment is constructed as:

$$x(k) = \begin{bmatrix} v(k) \\ r(k) \\ C_{\alpha fl} \\ C_{\alpha fr} \\ C_{\alpha rl} \\ C_{\alpha rr} \\ I_z \end{bmatrix} \tag{5-8}$$

$f(x(k), \theta)$ can be constructed according to eq. 2-15 and $h(x(k), \theta)$ takes the measurement value of v and r. After tuning, the measurement noise matrix R in lateral maneuver identification for Sample 1 is $\begin{bmatrix} 2 \times 10^{-1} & 0 \\ 0 & 2 \times 10^{-1} \end{bmatrix}$.

The state noise matrix Q is $\begin{bmatrix} 10^{-6} & 0 & 0 & 0 & 0 & 0 & 0 \\ 0 & 10^{-6} & 0 & 0 & 0 & 0 & 0 \\ 0 & 0 & 10^{-6} & 0 & 0 & 0 & 0 \\ 0 & 0 & 0 & 10^{-6} & 0 & 0 & 0 \\ 0 & 0 & 0 & 0 & 10^{-6} & 0 & 0 \\ 0 & 0 & 0 & 0 & 0 & 10^{-6} & 0 \\ 0 & 0 & 0 & 0 & 0 & 0 & 10^{-1} \end{bmatrix}$.

The measurement noise matrix R in lateral maneuver identification for Sample 2 is $\begin{bmatrix} 2 \times 10^{-2} & 0 \\ 0 & 2 \times 10^{-2} \end{bmatrix}$.

The state noise matrix Q is same as Q matrix for Sample 1.
The result for lateral maneuver is shown in Table 5-4

Parameter	$C_{\alpha fl}$	$C_{\alpha fr}$	$C_{\alpha rl}$	$C_{\alpha rr}$	I_z
Sample 1	51373	33596	35469	34302	1708
Sample 2	46904	39874	35822	32167	1806

Table 5-4: Lateral maneuver identification result for four wheels model

Validation The validation result is shown in Table 5-5

Sample 1 Validation					Sample 2 Validation				
Term	Value	RMSE	VAF(%)	Fig.	Term	Value	RMSE	VAF(%)	Fig.
$C_{\alpha fl}$	51373	130.22	96.5	5-13	$C_{\alpha fl}$	46904	58.96	99.3	5-14
$C_{\alpha fr}$	33596	155.13	95.1	5-15	$C_{\alpha fr}$	39874	67.70	99.1	5-16
$C_{\alpha rl}$	35469	70.01	97.5	5-17	$C_{\alpha rl}$	35822	62.40	98.0	5-18
$C_{\alpha rr}$	34302	50.00	98.8	5-19	$C_{\alpha rr}$	32167	57.41	98.4	5-20
I_z	1708	0.0058	99.3	5-21	I_z	1806	0.0049	99.5	5-22
System Identification: v		0.0022	98.0	5-23	System Identification: v		0.0023	97.8	5-24
System Identification: r		0.0158	99.4	5-23	System Identification: r		0.0095	99.8	5-24

Table 5-5: Lateral maneuver validation result for four wheels model in UKF identification

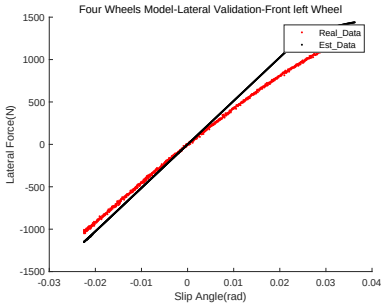

Figure 5-13: Driving Sample 1: Validation of $C_{\alpha fl}$ for four wheels model in UKF identification

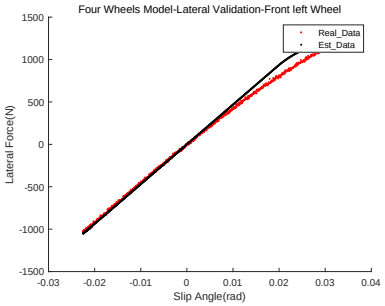

Figure 5-14: Driving Sample 2: Validation of $C_{\alpha fl}$ for four wheels model in UKF identification

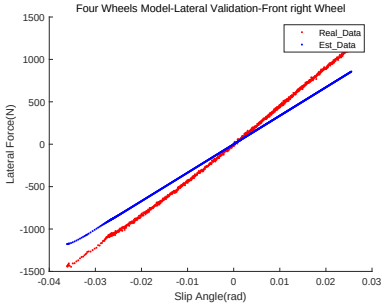

Figure 5-15: Driving Sample 1: Validation of $C_{\alpha fr}$ for four wheels model in UKF identification

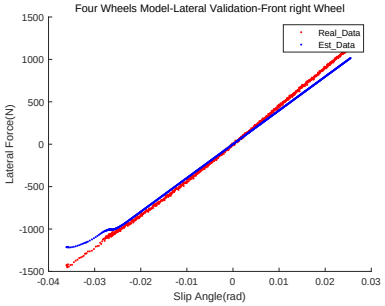

Figure 5-16: Driving Sample 2: Validation of $C_{\alpha fr}$ for four wheels model in UKF identification

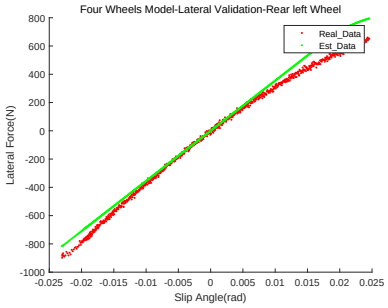

Figure 5-17: Driving Sample 1: Validation of $C_{\alpha rl}$ for four wheels model in UKF identification

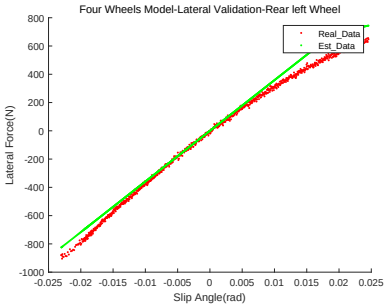

Figure 5-18: Driving Sample 2: Validation of $C_{\alpha rl}$ for four wheels model in UKF identification

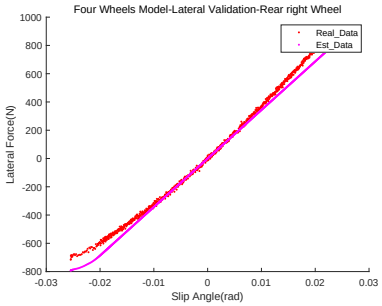

Figure 5-19: Driving Sample 1: Validation of $C_{\alpha rr}$ for four wheels model in UKF identification

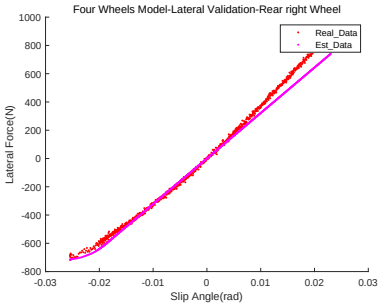

Figure 5-20: Driving Sample 2: Validation of $C_{\alpha rr}$ for four wheels model in UKF identification

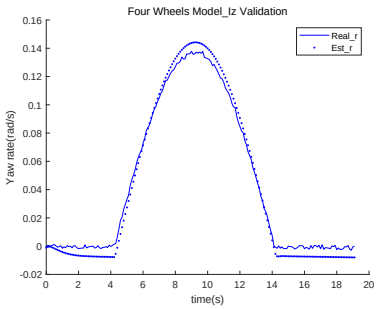

Figure 5-21: Driving Sample 1: Validation of I_z for four wheels model in UKF identification

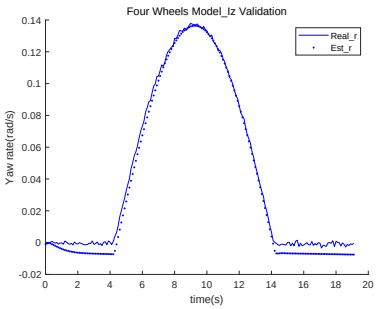

Figure 5-22: Driving Sample 2: Validation of I_z for four wheels model in UKF identification

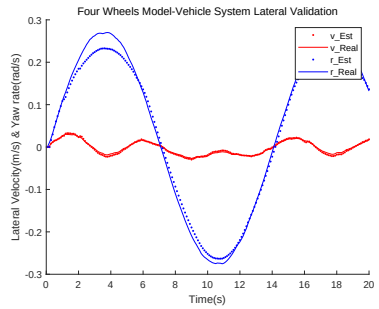

Figure 5-23: Driving Sample 1: System Validation of v and r for four wheels model in UKF identification

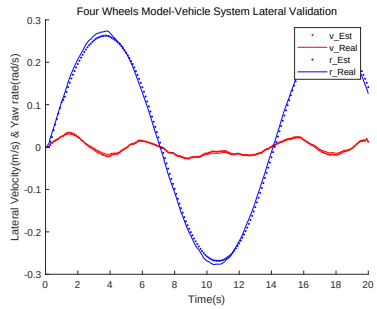

Figure 5-24: Driving Sample 2: System Validation of v and r for four wheels model in UKF identification

5-1-6 Discussion

After tuning, the validation result of the longitudinal maneuver is slightly worse than that of the Interior-point method, and the lateral result is slightly better than that of the Interior-point method. Overall, UKF can identify similar results as the Interior-point method, which means UKF can be used to identify nonlinear systems.
Unlike the Interior-point method, which optimizes the data of the whole time series, UKF optimizes and updates at each step. Thus lateral maneuver identification only costs 10 s, which is much lower than 36 s for the Interior-point method. In addition, UKF optimizes the state value by taking the minimum estimated covariance of the measured and the calculated quantity of the state.
The Interior-point method is suitable for off-line estimation, while UKF can also perform the on-line estimation. It is suitable for observing the system parameter that keeps changing. However, because each step updates the parameter state in a tiny amount, it is applicable to the system with slow parameter changing speed.
For off-line identification, the Interior-point method is more recommended than UKF. For one reason, UKF introduces new parameters: measurement and state noise covariance matrices Q and R. For the system state, under the condition of accurate model, different R and Q matrices will not have a dramatic impact on the final state. But this is not the case for parameter identification. Since parameters have the coupling effect, there are many local optimum for the identification. For UKF, the different choices of R and Q matrices will affect the point to which the system converges. As shown in Table 5-3, the validation result for Sample 2 identification has a significant deviation, but the system identification shows a good result with VAF of 99.7%. Therefore, for different data sets, it is necessary to manually adjust the R and Q matrix value so that the final result can converge to real value. Although the value of the matrix is within an approximate range and does not need to be particularly precise, the manual tuning still consumes time and reduces the autonomy of the system.
In the longitudinal identification, the results of Sample 1 are much inferior to those of Sample 2 for UKF identification. More experiments in this project also show that UKF has a large deviation for different samples and also for different R and Q matrices, so UKF identification stability is relatively inferior and also requires more manual tuning time. Therefore, to automatically complete the identification, the PSO-UKF in the next section will attempt to find the appropriate covariance matrix.

5-2 Particle Swarm Optimization - Unscented Kalman Filter Identification

5-2-1 Particle Swarm Optimization Algorithm

Particle Swarm Optimization (PSO) algorithm is a global random search algorithm, which was inspired by the migration and clustering behaviors during the foraging of birds.
In PSO, each particle is like a bird in the search space. All particles have a fitness value determined by the optimized function, and each particle has a speed that determines the direction and distance they fly.
PSO initially construct a group of random particles and then iterated to find the optimal solution. In each iteration, the particle updates itself by tracking two best solutions; The first is the personal best found by the particle itself; The other best is the common best experience among the members.
The procedures are shown below:

1. *Initialization.* Initialize a population of particles with a population size of M in the search space. Each individual in the population includes position $x_i(t)$ and velocity $v_i(t)$.

2. *Individual and global optimum calculation.* According to the fitness function, the personal best is updated by the best position found for each particle, marked as $p_i(t)$. The common best is updated by the best value from these personal best solutions, which is marked as $g(t)$.

3. *Velocity and position updating.* Calculate the new speed for each individual by the personal best and common best positions as the following formula:

$$v_i(t+1) = wv_i(t) + c_1r_1(p_i(t) - x_i(t)) + c_2r_2(g(t) - x_i(t)) \tag{5-9}$$

   where w is inertia weight.
   c_1 and c_2 are learning factors, also known as acceleration constant.
   r_1 andr_2 are random numbers within $[0, 1]$.

   In equation 5-9, the first part represents the influence of the previous velocity of the particle to ensure the global convergence of the algorithm. The second part and the third part gives the algorithm have local convergence possibility. It can be seen that the inertial weight w in equation 5-9 indicates to what extent the original velocity is retained. Large w means strong global convergence possibility and weak local convergence possibility; Small w means strong local convergence possibility, weak global convergence possibility.
   Then, the new position for each individual can be calculated as:

$$x_i(t+1) = x_i(t) + v_i(t+1) \tag{5-10}$$

4. *Termination.* The iteration will be terminated when the maximum iteration number is reached or the difference between the best value of two consecutive iteration is less than the threshold.

5-2-2 PSO-UKF

One crucial problem of UKF is that the performance of its system is affected by measurement noises covariance matrix R and state noises covariance matrix Q. R and Q matrices are generally difficult to know when making system identification at the beginning. It is necessary to manually adjust the parameters of the two according to the error, but this makes the system less autonomous and consumes more time. Therefore, it is worth exploring to optimize the Q and R parameters of UKF through PSO [2].
The block diagram of this method is shown in Fig. 5-25.

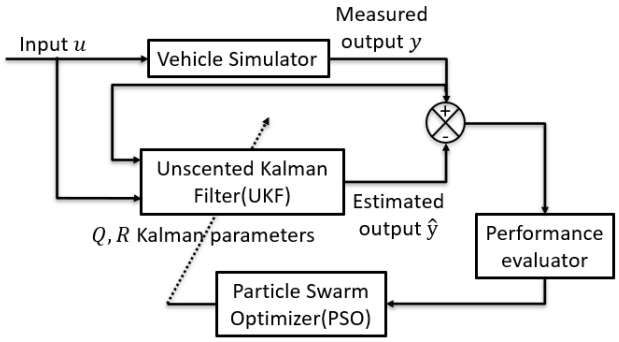

Figure 5-25: Block diagram of PSO-UKF parameter estimation system [2]

The Performance evaluator will evaluate the performance of UKF by using the current Q and R matrices, and send it to PSO. Base on the evaluation result, PSO will update Q and R matrices by the algorithm introduced in Section 5-2-1. The new matrices will be used for the adaptation of the UKF for the next iteration until the maximum number of iteration reached and optimum obtained [2].

5-2-3 Identification by PSO-UKF

The size of R and Q matrices determine the reliability of the measured value and the state calculated value. The larger R is, the greater the noise of the measured value is, the lower the reliability is, and vice versa. When the R value is small, and the measurement reliability is high, the prediction depends more on the quantity of measurement than the quantity of state calculation. Q and R matrices can be estimated by PSO-UKF.

Parameters Identification This method is tried on lateral maneuver because the model is relatively complex, it can better reflect the quality of the algorithm. The better data set Sample 2 for lateral maneuver are used in this identification.
The convergence of the PSO depends on the initial points and its parameters c_1, c_2 and w. The values of these parameters are defined as follows: $c_1 = 2$, $c_2 = 2$ and $w = 0.5$ [2]. The value of initial points of PSO are chosen from 10^{-1} to 10^{-5}. The result Q matrix is

$$\begin{bmatrix} 4.2\times10^{-2} & 0 & 0 & 0 & 0 & 0 & 0 \\ 0 & 4.4\times10^{-2} & 0 & 0 & 0 & 0 & 0 \\ 0 & 0 & 4.5\times10^{-2} & 0 & 0 & 0 & 0 \\ 0 & 0 & 0 & 4.6\times10^{-2} & 0 & 0 & 0 \\ 0 & 0 & 0 & 0 & 4.2\times10^{-2} & 0 & 0 \\ 0 & 0 & 0 & 0 & 0 & 4.3\times10^{-2} & 0 \\ 0 & 0 & 0 & 0 & 0 & 0 & 4.2\times10^{-2} \end{bmatrix}.$$

The result R matrix is $\begin{bmatrix} 1e-4 & 0 \\ 0 & 1e-4 \end{bmatrix}$.

Take R and Q matrices into UKF, the estimated parameters are shown in Table 5-6.

Parameter	$C_{\alpha fl}$	$C_{\alpha fr}$	$C_{\alpha rl}$	$C_{\alpha rr}$	I_z
Value	69279	12920	33872	31686	725

Table 5-6: Lateral maneuver identification result for four wheels model in PSO-UKF identification

Validation The validation result is shown in Table 5-7

Sample 2 Validation				
Term	Value	RMSE	VAF(%)	Fig.
$C_{\alpha fl}$	69279	337.10	76.9	5-26
$C_{\alpha fr}$	12920	491.53	51.1	5-27
$C_{\alpha rl}$	33872	66.45	97.7	5-28
$C_{\alpha rr}$	31686	61.59	98.1	5-29
I_z	725	0.1023	0	5-30
System Identification: v		0.0146	13.4	5-31
System Identification: r		0.0217	98.8	5-31

Table 5-7: Longitudinal maneuver validation result for four wheels model in PSO-UKF identification

5-2-4 Discussion

After many experiments, the results obtained by PSO-UKF are worse than UKF. Since each point needs to be computed multiple times UKF for iteration. The running time of one point for one iteration is about 1 second, and the identification needs 15 minutes for 9 initial points and 200 iterations. Compared with the Interior-point method and UKF, the time cost is dramatically increased, and the result accuracy cannot be guaranteed. One reason is that PSO needs dozens or even hundreds of initial points and thousands of iterations to find the optimal solution in such dimension. But the time cost is too high.

On the other hand, PSO-UKF uses the difference between the measured value and the estimated value for evaluation, but it cannot eliminate the influence of noises. Therefore, PSO-UKF tends to make the R matrix as low as possible to ensure that the estimated value is the same as the measured value with noises, which leads to the inaccuracy of the final result.

However, this method can be used to make a prediction without knowing the magnitude of parameters to be identified as a reference.

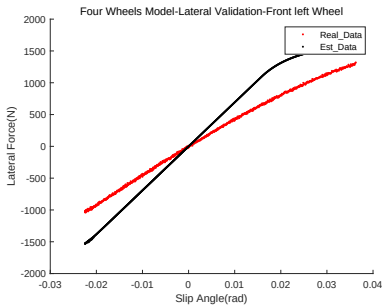

Figure 5-26: Driving Sample 2: Validation of $C_{\alpha fl}$ for four wheels model in PSO-UKF identification

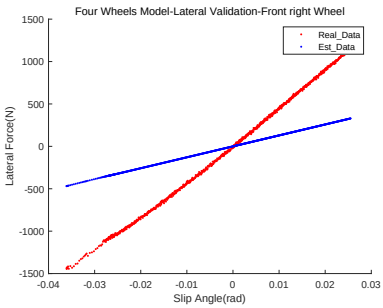

Figure 5-27: Driving Sample 2: Validation of $C_{\alpha fr}$ for four wheels model in PSO-UKF identification

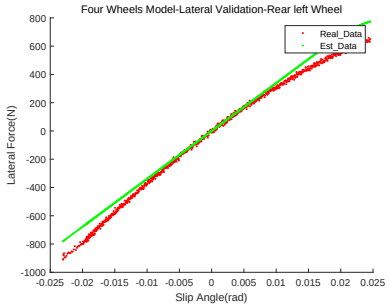

Figure 5-28: Driving Sample 2: Validation of $C_{\alpha rl}$ for four wheels model in PSO-UKF identification

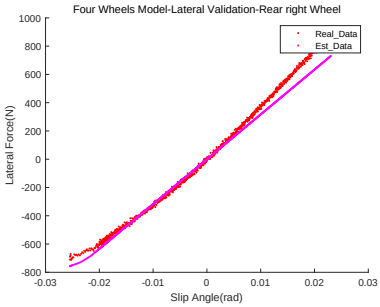

Figure 5-29: Driving Sample 2: Validation of $C_{\alpha rr}$ for four wheels model in PSO-UKF identification

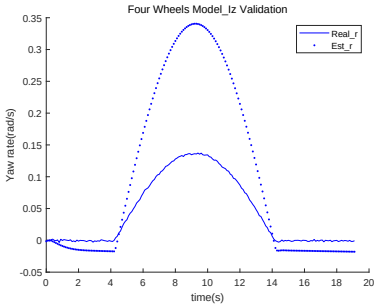

Figure 5-30: Driving Sample 2: Validation of I_z for four wheels model in PSO-UKF identification

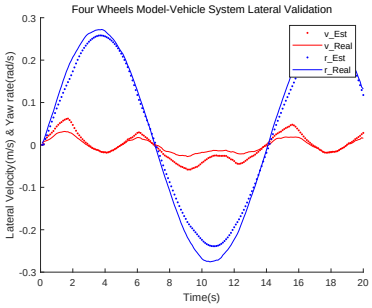

Figure 5-31: Driving Sample 2: System Validation of v and r for four wheels model in PSO-UKF identification

5-3 Genetic Algorithm Identification

5-3-1 Genetic Algorithm

GA is a computational model of biological evolution that simulates the natural selection and laws of natural genetics. It is a method to search for the optimal solution by simulating the natural evolution process.
A GA starts with a population that represents a possible collection of potential solutions to a problem, while a population consists of individuals encoded by genes. As the main carrier of genetic, chromosome is a collection of multiple genes, and its internal expression determines the external expression of an individual.
The introduction of GA reference the paper "An Alternative Method to Determine the Magic Tyre Model Parameters Using Genetic Algorithms" [3].
The optimization problem is given by:

$$\begin{aligned} &min\ f(X) \\ &subject\ to: \\ &g_i(X) \leq 0\ j = 0, 1, 2, \ldots, m \\ &x_i \in [li_i, ls_i]\ \forall x_i \in X \end{aligned} \tag{5-11}$$

where $f(\cdot)$ is the goal function, where each individual X can obtain its fitness value from it. $g_i(\cdot)$ are the constraints defining the search space.
This optimization method begins with a set of starting population, where each individual (chromosome) randomly generates a set of parameters (genes) in identification system representing a possible solution.
Each gene x_i can be expressed by binary code of of size p [32] which determines the precision of each gene and the range is within $[li, ls]$.
Next, the initial population must evolve into a population where each individual has a better solution. This can be done through natural selection, reproduction, mutation or other genetic operations. Selection and reproduction are carrier out sequentially, and mutation is an independent process [3].

Selection In terms of selection, usually two individuals are randomly selected as parents from the population to form a couple for reproduction. The weight of each individual depends on its fitness, so the best individual has the greatest probability of being chosen.
In this project, the selection method references Storn and Price [33], known as differential evolution. One parent V is the combination of two randomly selected individuals and the best individual, shown as following:

$$V = X_{best} + F \cdot (X_{r1} - X_{r2}) \tag{5-12}$$

where X_{best} is the best individual of a population, X_{r1} and X_{r2} are two randomly selected individuals, and F is set as 0.4 that controls the disturbance of the best individual.
Another parent X_i is randomly selected from population with probability.

Reproduction Next, two parents V and X_i will reproduce its descendant through crossover, which interchange part of genes from parent individuals to form the descendant genes. The schematic diagram of crossover is shown in Fig. 5-32

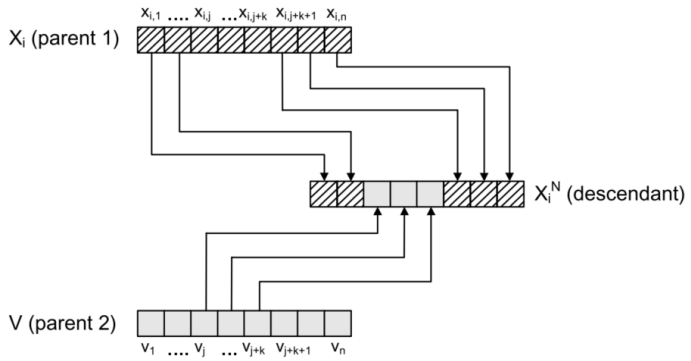

Figure 5-32: Piecewise multi-point crossover for reproduction [3]

The crosing points, $(j, j+k)$, are randomly selected.
The new descendant X_i^N will be kept only if its fitness is better than its antecedent X_i, otherwise, X_i is retained. Crossover is carried out with a probability defined as $CP \in [0, 1]$. CP is set as 0.6 in this project.

Mutation Mutation is the value of certain genes on chromosome changes according to the characteristics of the coding. In binary coding, some position on the gene changes from "0" to "1" or "1" to "0". Mutation happens with a small probability defined as $MP \in [0, 1]$ which is much lower than CP. MP is set as 0.6 in this project.
The flow chart of GA is shown in Fig. 5-33
GA is used in this section to identify the parameters of the magic formula.
According to Subsection 2-1-1, the goal function can be set as [3]:

$$\min_{PARA} \sum_{i=1}^{n} [Y^*_{combined}(X_i) - Y_{measured}(X_i)]^2$$
$$where\ X_i = \{\alpha_1, \alpha_2, \ldots, \alpha_i\} \vee X_i = \{\lambda_1, \lambda_2, \ldots, \lambda_i\}$$
$$and\ PARA = \begin{Bmatrix} PDX1, PDX2, PCX1, PEX1, PEX2, PEX3, PEX4, PKX1, PKX2, \\ PKX3, PHX1, PHX2, PVX1, PVX2, RCX1, RBX1, RBX2, RHX1 \end{Bmatrix} \vee$$
$$\begin{Bmatrix} PDY1, PDY2, PCY1, PEY1, PEY2, PEY3, PKY1, \\ PKY2, PHY1, PHY2, PVY1, PVY2, RCY1, RBY1, \\ RBY2, RBY3, RHY1, RVY1, RVY2, RVY4, RVY5, RVY6 \end{Bmatrix} \rightarrow Y^*_{combined} \tag{5-13}$$

Identification This algorithm is firstly tried in lateral maneuver identification and the data is the same one used in Interior-point identification part.

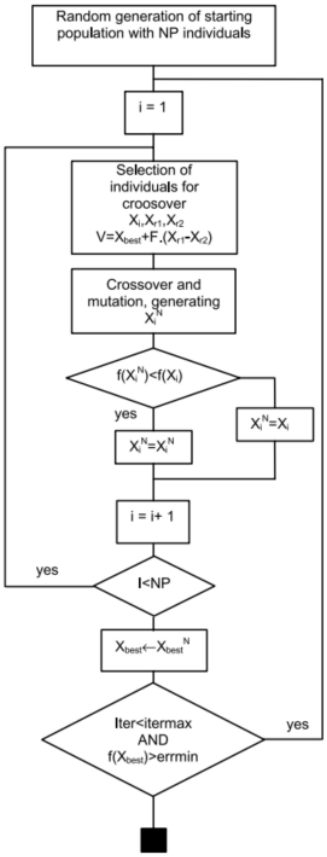

Figure 5-33: Scheme of the entire algorithm of genetic algorithm [3]

Due to the large parameter dimension, the lateral force F_y is used directly. The result for one tire is shown in Table 5-8

Parameter	Value	Parameter	Value	Parameter	Value
PDY1	-1.059	PDY2	0.064	PCY1	0.223
PEY1	-2.529	PEY2	0.200	PEY3	-0.531
PKY1	-18.29	PKY2	3.99	PHY1	0.060
PHY2	-0.053	PVY1	0.280	PVY2	-0.090
RCY1	4.098	RBY1	9.321	RBY2	7.661
RBY3	-0.245	RHY1	0.296	RVY1	0.301
RVY2	-0.079	RVY4	11.204	RVY5	4.869
RVY6	-54.376				

Table 5-8: Identified parameters of Magic Formula

Validation The lateral force calculated by the identified parameters compares with measured data. The plot is shown in Fig. 5-34

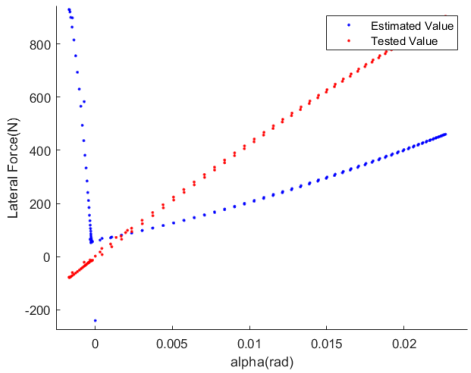

Figure 5-34: Magic Formula Validation

5-3-2 Discussion

This experiment shows that in the case of vehicle driving maneuver, it is challenging to identify Magic Formula. The main reason is that Magic Formula has more than 20 parameters. Each dimension requires multiple values to find the global optimal solution. Even assuming two values for each dimension, that would require 2^{20}, nearly a million different combinations. It remains challenging to optimize through selection, mutation, and crossover. As a result, the parameters identified in the end deviate significantly from the real value, and it is not easy to find the global optimal solution in this dimension. Therefore, it is necessary to reduce the dimension of the system before the optimization calculation. In general, when the tire vertical load is constant, the parameter B,C,D and E are also constant. At this time, if different slip angles and their generated lateral forces can be obtained, B,C,D and E can be identified first, and then the corresponding sub-parameters can be identified respectively. This method can reduce parameter identification of more than 20 dimensions to 4 dimensions. However, in the vehicle driving maneuver, the longitudinal force of each tire of the vehicle changes as the driving angle changes, and it cannot be controlled to keep constant. So Magic Formula is not suitable for use in this situation. Relatively speaking, the Dugoff model can simulate the tire model well under the condition of stable operation of most cases, and the number of parameters is greatly reduced, which can make the model establishment more accurate, so it is a very efficient choice.

5-4 Conclusion

This chapter attempts several identification methods, including UKF, PSO-UKF and GA. UKF results are close to the Interior-point method, but due to the introduction of noise covariance matrices, which needs to be tuned. This increases the time consumption for manually tuning, uncertainty and reduces the autonomy of identification system. Since UKF can estimate at each time step, it is very suitable for on-line system identification and parameter estimation. For off-line identification, the Interior-point method is a better choice. PSO-UKF is used to adjust the noise covariance matrices automatically, but because PSO needs dozens of initial points and hundreds or even thousands of iteration times, which means UKF identification process needs to be calculated thousands of times and consume a scary amount of

time. In the case of a small number of initial points and iterations, the result of PSO-UKF is greatly influenced by initial points. When the choice of initial points are far from the optimal solution, PSO-UKF is difficult to converge. Finally, we try to identify a more accurate Magic Formula tire model by GA. In the case of vehicle tests, it is difficult to keep the vertical force constant with changing steering angle, so effectively reduce the dimension is very difficult. GA at this time directly dealing with the Magic Formula tire model is not capable of. The above experiments are the algorithm comparisons of the Interior-point method.

Chapter 6

Conclusions and Recommendations

This chapter summarizes the vehicle's overall system identification in three aspects: data set, model, and algorithm selection. The areas for further exploration and improvement will also be suggested.

6-1 Conclusions

A good vehicle identification result mainly needs three key elements: proper data set, an accurate vehicle model, and an efficient algorithm. These three elements are also be selected and optimized by validation results. The vehicle identification cycle's key elements are shown in Fig. 6-1. The following conclusion about this thesis is also divided into these aspects.

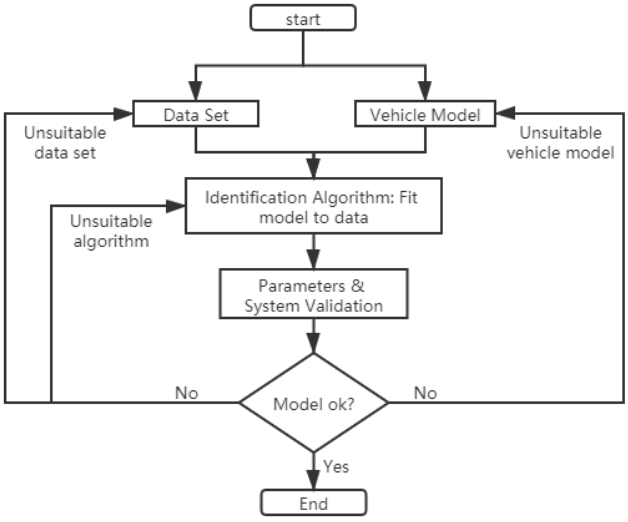

Figure 6-1: A schematic view of the key elements in vehicle identification cycle [4]

6-1-1 Data Set Selection

In the experiments of the Interior-point algorithm and Unscented Kalman Filter (UKF), there are two data sets involved in the identification for both longitudinal and lateral maneuver. The identification result of Sample 2 is often better than that of Sample 1. By comparing the results of these two samples, some conclusions and suggestions for data set selection can be drawn. The system validation results of Sample 1 are usually excellent, but the errors of parameter identification results are substantial. There are two main reasons, the coupling of parameters and lack of 'excitation' in parameter identification. Parameter coupling, such as between C_α and I_z, the error calculated from both parameters cancels out in estimation. One way to solve this problem is to add constraints to the parameters. When there are no new restrictions, the selected data set should have persistency of excitation, where the data set is multi-frequency oscillation, and the identification parameters are easier to converge to the true value.
If the influence of parameters on the system is more significant, the identification accuracy will be higher. The air resistance increases with the quadratic speed, where the resistance is small at low speed and becomes large at high speed. When the influence of air resistance on the system is small, the identification error would be more extensive. Therefore, the longitudinal maneuver identification error of Sample 1 is greater than that of Sample 2. So the right data set needs to be chosen according to the characteristics of the parameters.

6-1-2 Model Selection

The establishment of a vehicle model is a crucial step in vehicle's system identification, including the selection of vehicle mathematical model, vehicle subsystem model, and sensor.
The complexity of model selection is determined according to the requirements of identification, and the accuracy of a complex system is usually better than that of a simple system. However, overly complex systems introduce unknown parameters, which may cause parameter coupling. Decoupling needs an enormous computational load and more sensors. After the previous experiment, the four wheels model has the right balance between the calculation amount and accuracy. The dynamic performance of the system can be well described by establishing the relationship between forces and accelerations or inertia through differential equations. The bicycle model has a good performance in longitudinal identification, while the error in lateral identification is larger. This result can meet the requirements of low precision tasks. Identification took 13 s, about a third as long as the four wheels model. For the system with strict calculation amount requirements, the calculation amount of the bicycle model will be much less. By comparing the results of Sample 1 and Sample 2, it can be seen that the bicycle model can get quite different results for different data sets, so its selection of data sets should be more rigorous.
The tire model is a mathematical expression based on theoretical calculation and practice. The accurate model is the Magic Formula, but the Magic Formula is not suitable for this project because of the excessive number of parameters. The Dugoff model also provides a model to balance accuracy and computational effort in situations where it is impossible to disassemble a tire for separate simulation experiments. The simplified linear model is suitable for stable and gentle driving maneuver, which will cause a large error if the force caused by slip is in a saturation stage.

6-1-3 Algorithm Selection

The algorithm should also have the advantages of less computational load and higher precision. The Interior-point nonlinear optimization algorithm method is chosen because it can find the best parameter set at a fast speed and with decent accuracy. Moreover, it can do the optimization of the data over the whole time cycle. Identification by UKF, approximate results can be obtained, and the computation time is about one-third of the Interior-point method. However, since UKF introduces new algorithm variables, R and Q matrices. For each data set, manual tuning of the matrices is needed to avoid local optimum, which significantly increases the human effort and the time to construct a proper identification system. By comparing Sample 1 and Sample 2, it can also be found that UKF produces extensive difference identification results for different data sets, so the stability is worse than that of the Interior-point method. Particle Swarm Optimization-Unscented Kalman Filter (PSO-UKF) makes the system automatically adjust the parameters, but its low accuracy and long computation time make it no advantage over the Interior-point method. However, UKF is suitable for on-line identification of slowly changing or constant parameters. For the off-line identification of vehicles in this project, the Interior-point method is a better choice. The project tried to identify the parameters of the Magic Formula with Genetic Algorithm (GA). It turns out that while the Magic Formula is suitable for finding the optimum in the non-convex and multidimensional system, it still fails to deal with the dimension of the Magic Formula.

6-2 Recommendations

6-2-1 Identification in Less Stable Condition

This project is mainly carried out experiments at low speed with a large steering angle or high speed with a small steering angle, not much considering the state of parameters when tire forces are saturated under drifting or out of control conditions. Research in this area can improve vehicle safety in extreme environments and conditions.

6-2-2 Parameters Decoupling

Parameter coupling is a difficult problem to solve in system identification. When the observable states are far less than the unknown parameters, parameter coupling often occurs. For example, air resistance and tire longitudinal force will affect the vehicle's longitudinal movement, which is difficult to be separated. In general, solving parameter coupling can increase the mathematical relationship between the parameters of the model, thus increasing the limitation. Alternatively, add observable quantities, such as air resistance sensors, or use data sets with the persistence of excitation. However, all approaches have limitations, such as some models cannot be constructed more mathematical relations, and the cost of adding observers or sensors is too high. In this case, how to decouple the parameters is a necessary research direction.

Bibliography

[1] Hans Pacejka. *Tire and vehicle dynamics*. Elsevier, 2005.

[2] Yahia Laamari, Kheireddine Chafaa, and Belkacem Athamena. Particle swarm optimization of an extended kalman filter for speed and rotor flux estimation of an induction motor drive. *Electrical Engineering*, 97(2):129–138, 2015.

[3] JA Cabrera, A Ortiz, E Carabias, and A Simon. An alternative method to determine the magic tyre model parameters using genetic algorithms. *Vehicle system dynamics*, 41(2):109–127, 2004.

[4] Michel Verhaegen and Vincent Verdult. *Filtering and system identification: a least squares approach*. Cambridge university press, 2007.

[5] Graham C Goodwin, Stefan F Graebe, Mario E Salgado, et al. *Control system design*. Upper Saddle River, NJ: Prentice Hall,, 2001.

[6] Petre Stoica and Torsten Söderström. System identification. *Prentice-Hall International*, 1989.

[7] M Bayani Khaknejad, R Kazemi, Sh Azadi, and A Keshavarz. Identification of vehicle parameters using modified least square method in adams/car. In *Proceedings of 2011 International Conference on Modelling, Identification and Control*, pages 98–103. IEEE, 2011.

[8] XY Liu, Stefano Alfi, and Stefano Bruni. An efficient recursive least square-based condition monitoring approach for a rail vehicle suspension system. *Vehicle System Dynamics*, 54(6):814–830, 2016.

[9] Thomas A Wenzel, KJ Burnham, MV Blundell, and RA Williams. Dual extended kalman filter for vehicle state and parameter estimation. *Vehicle system dynamics*, 44(2):153–171, 2006.

[10] Emmanuel D Blanchard, Adrian Sandu, and Corina Sandu. Parameter estimation method using an extended kalman filter. 2007.

[11] Pepijn WJ Van De Ven, Tor A Johansen, Asgeir J Sørensen, Colin Flanagan, and Daniel Toal. Neural network augmented identification of underwater vehicle models. *Control Engineering Practice*, 15(6):715–725, 2007.

[12] Alireza Alfi and Mohammad-Mehdi Fateh. Intelligent identification and control using improved fuzzy particle swarm optimization. *Expert Systems with Applications*, 38(10):12312–12317, 2011.

[13] Péter Baranyi. Carsim. https://www.carsim.com/products/carsim.

[14] Rajesh Rajamani. *Vehicle dynamics and control*. Springer Science & Business Media, 2011.

[15] Howard Dugoff, Paul S Fancher, and Leonard Segel. An analysis of tire traction properties and their influence on vehicle dynamic performance. *SAE transactions*, pages 1219–1243, 1970.

[16] G Gim and PE Nikravesh. An analytical study of pneumatic tire dynamic properties. part 1–3. *International Journal of Vehicle Design*, 11(6):589–618, 1991.

[17] Hans B Pacejka and Egbert Bakker. The magic formula tyre model. *Vehicle system dynamics*, 21(S1):1–18, 1992.

[18] P Bayle, JF Forissier, and S Lafon. A new tyre model for vehicle dynamics simulations. *Automotive Technology International*, 93:193–198, 1993.

[19] Mingyuan Bian, Long Chen, Yugong Luo, and Keqiang Li. A dynamic model for tire/road friction estimation under combined longitudinal/lateral slip situation. Technical report, SAE Technical Paper, 2014.

[20] Howard Dugoff. Tire performance characteristics affecting vehicle response to steering and braking control inputs. final report. Technical report, 1969.

[21] Giulio Reina, Matilde Paiano, and Jose-Luis Blanco-Claraco. Vehicle parameter estimation using a model-based estimator. *Mechanical Systems and Signal Processing*, 87:227–241, 2017.

[22] Mechanical Simulation. Carsim data manual, 2011.

[23] Stephen Boyd, Stephen P Boyd, and Lieven Vandenberghe. *Convex optimization*. Cambridge university press, 2004.

[24] Richard H Byrd, Mary E Hribar, and Jorge Nocedal. An interior point algorithm for large-scale nonlinear programming. *SIAM Journal on Optimization*, 9(4):877–900, 1999.

[25] Iven Mareels. Sufficiency of excitation. *Systems & control letters*, 5(3):159–163, 1984.

[26] Jan C Willems, Paolo Rapisarda, Ivan Markovsky, and Bart LM De Moor. A note on persistency of excitation. *Systems & Control Letters*, 54(4):325–329, 2005.

[27] Charles K Chui, Guanrong Chen, et al. *Kalman filtering*. Springer, 2017.

[28] Eric A Wan and Rudolph Van Der Merwe. The unscented kalman filter for nonlinear estimation. In *Proceedings of the IEEE 2000 Adaptive Systems for Signal Processing, Communications, and Control Symposium (Cat. No. 00EX373)*, pages 153–158. Ieee, 2000.

[29] Sanghyun Hong, Tory Smith, Francesco Borrelli, and J Karl Hedrick. Vehicle inertial parameter identification using extended and unscented kalman filters. In *16th International IEEE Conference on Intelligent Transportation Systems (ITSC 2013)*, pages 1436–1441. IEEE, 2013.

[30] Lennart Ljung. Asymptotic behavior of the extended kalman filter as a parameter estimator for linear systems. *IEEE Transactions on Automatic Control*, 24(1):36–50, 1979.

[31] Michele Russo, Riccardo Russo, and Agsotino Volpe. Car parameters identification by handling manoeuvres. *Vehicle System Dynamics*, 34(6):423–436, 2000.

[32] John H Holland. Genetic algorithms and the optimal allocation of trials. *SIAM Journal on Computing*, 2(2):88–105, 1973.

[33] Rainer Storn and Kenneth Price. Differential evolution–a simple and efficient heuristic for global optimization over continuous spaces. *Journal of global optimization*, 11(4):341–359, 1997.

Glossary

List of Acronyms

KF	Kalman Filter
UKF	Unscented Kalman Filter
PSO	Particle Swarm Optimization
PSO-UKF	Particle Swarm Optimization-Unscented Kalman Filter
GA	Genetic Algorithm
COG	center of gravity
RMSE	Root Mean Square Error
VAF	variance accounted for